PUBLICATIONS OF THE ASTRONOMICAL SOCIETY OF THE PACIFIC, **118**:183–204, 2006 February

Invited Review

The Elemental Abundances in Bare Planetary Nebula Central Stars and the Shell Burning in AGB Stars

KLAUS WERNER

Institut für Astronomie und Astrophysik, Universität Tübingen, Sand 1, D-72076 Tübingen, Germany; werner@astro.uni-tuebingen.de

AND

FALK HERWIG

Theoretical Astrophysics Group, Los Alamos National Laboratory, Mail Stop B227, Los Alamos, NM 87545; fherwig@lanl.gov

Received 2005 December 12; accepted 2005 December 12; published 2006 February 24

ABSTRACT. We review the observed properties of extremely hot, hydrogen-deficient post–asymptotic giant branch (AGB) stars of spectral type [WC] and PG1159. Their H deficiency is probably caused by a (very) late helium-shell flash or an AGB final thermal pulse, laying bare interior stellar regions that are usually kept hidden below the hydrogen envelope. Thus, the photospheric elemental abundances of these stars allow us to draw conclusions about details of nuclear burning and mixing processes in the precursor AGB stars. We summarize the state of the art of stellar evolution models that simulate AGB evolution and the occurrence of a late He-shell flash. We compare predicted elemental abundances to those determined by quantitative spectral analyses performed with advanced non-LTE model atmospheres. Good qualitative and quantitative agreement is found. Future work can contribute to an even more complete picture of the nuclear processes in AGB stars.

Online material: color figures

1. INTRODUCTION

Post–asymptotic giant branch (AGB) stars represent a relatively short-lived transition phase between AGB stars and white dwarf (WD) stars. All stars with initial masses between 1 and ~8 $M_\odot$ become H- and He-shell burning AGB stars and end their lives as WDs with a carbon-oxygen core. The model evolution is shown in Figure 1 for initial masses of 2 $M_\odot$. More massive, super-AGB stars up to 12 $M_\odot$ may end as ONeMg WDs. During the hottest phases, post-AGB stars are surrounded by a planetary nebula (PN), ionized material lost by the precursor AGB star. Canonical stellar evolution predicts that throughout all evolutionary phases these stars retain hydrogen-rich envelopes that can, however, become contaminated by processed material from the interior by dredge-up events occurring in the red giant branch (RGB) and AGB stages. Such an evolution is described by the solid line in Figure 1.

Decades ago, the observation of central stars of planetary nebulae (CSPNs) exhibiting emission-line spectra, which are very similar to those of massive Wolf-Rayet stars with strong helium and carbon emission lines (i.e., spectral type [WC]), suggested the existence of hydrogen-deficient post-AGB stars (e.g., Heap 1975). Later, the Palomar-Green survey revealed a new spectral class of H-deficient post-AGB stars, the PG1159 stars, which are dominated by absorption lines of highly ionized He, C, and O (Wesemael et al. 1985). It is now believed that the PG1159 stars are descendants of the Wolf-Rayet CSPNs and that the majority of them will evolve into WDs with helium atmospheres (i.e., non-DA white dwarfs).

The origin of the hydrogen deficiency in [WC] and PG1159 stars is probably a late helium-shell flash, which means that a post-AGB star (or WD) reignites helium-shell burning and transforms the star back into an AGB star. This "born-again AGB star" phenomenon was discovered in early stellar evolution modeling (Fujimoto 1977; Schönberner 1979) and was later invoked to explain the H deficiency observed in some hot post-AGB stars (Iben et al. 1983; Herwig et al. 1999). A complete evolutionary track of such a born-again evolution is shown as the dashed line in Figure 1. The late He-shell flash causes complete envelope mixing. Hydrogen is ingested and burned, and the surface chemistry of the star becomes dominated by the composition of the previous He/C/O-rich intershell layer (the region between the H- and He-burning shells of the AGB star; see § 3.1).

In "usual," i.e., hydrogen-rich (post-) AGB stars, intershell matter can be dredged up to the surface (the so-called third dredge-up) and results in the pollution of the photosphere with intershell matter; that is, helium, 3α-burning products (C, O, and Ne), and *s*-process elements produced by neutron capture in the He-burning environment. The study of *s*-process elemental abundances in AGB stars was and is the most important tool for revealing details of the physics of burning and mixing processes. It is essential to the understanding of these processes,

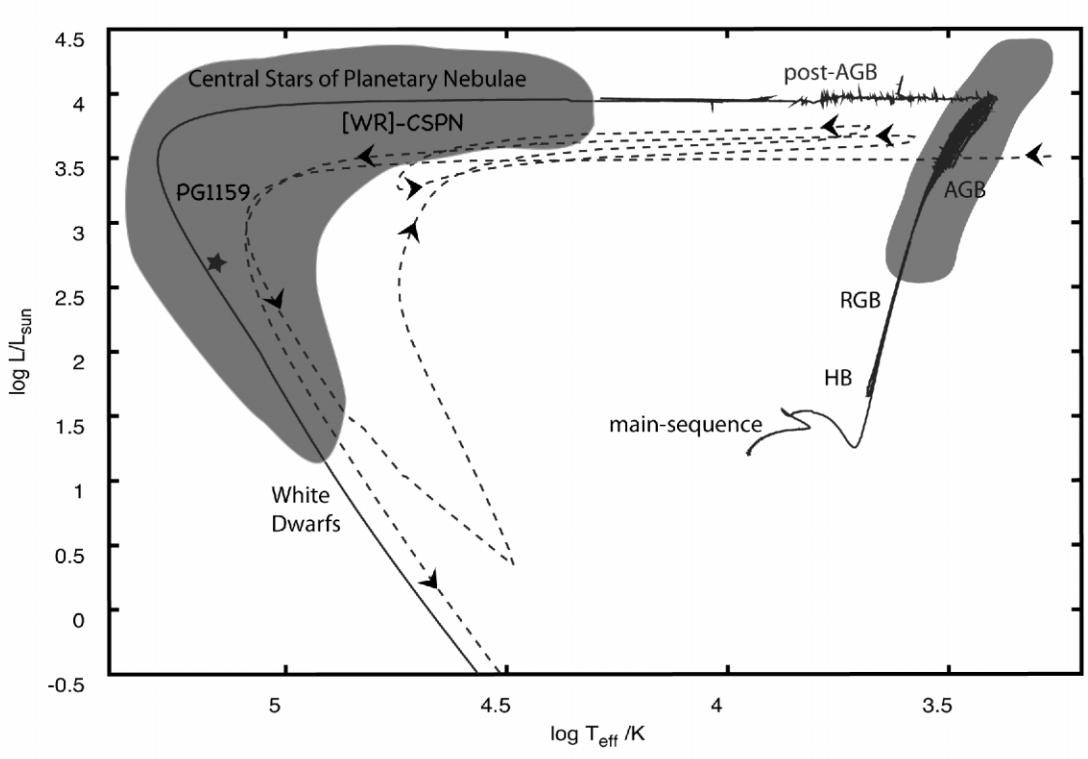

FIG. 1.—Complete stellar evolutionary track with an initial mass of 2 $M_{\odot}$ from the main sequence through the RGB phase, the horizontal-branch phase to the AGB phase, and finally through the post-AGB phase, which includes the CSPNs to the final white dwarf stage. The solid line represents the evolution of a H-normal post-AGB star. The dashed line shows a born-again evolution of the same mass, triggered by a very late thermal pulse, although shifted by approximately $\Delta \log T_{\rm eff} = -0.2$ and $\Delta \log (L/L_{\odot}) = -0.5$ for clarity. The five-pointed star shows the position of PG 1159−035. (Reprinted with permission, and with minor modifications, from Herwig 2005.)

because they affect the yields from AGB stars, which largely drive the chemical evolution of the Galaxy.

In contrast to these H-rich stars, [WC] and PG1159 stars not only exhibit traces of intershell matter in their photospheres, they are in fact essentially made up of intershell matter. This is because the mass of the intershell is much larger than that of the hydrogen envelope, and thus its composition dominates the mixture of both layers triggered by the late He flash. These H-deficient post-AGB stars therefore offer the unique possibility of studying intershell abundances *directly* and hence understanding the physical processes leading to the composition.

2. QUANTITATIVE SPECTRAL ANALYSES

In this section we summarize results from spectral analyses. We focus on PG1159 stars (§ 2.1), because we think that in particular the abundance analyses for many species is very advanced for this spectral subclass. We then turn to the [WC] central stars (§ 2.2), with emphasis on evidence for the evolutionary link with the PG1159 stars. Both [WC] and PG1159 stars are thought to result from a late He-shell flash, although this is still debated. We later discuss observations that appear to challenge the "born-again" scenario, and we touch upon alternative ideas. In any case, these stars are obviously exhibiting intershell matter and thus are of immediate interest for gaining insight into AGB evolution.

Besides [WC] and PG1159 stars, there exist several other spectroscopic subclasses of H-deficient post-AGB stars that certainly cannot be explained by the "born-again" scenario. These subtypes comprise R Coronae Borealis (RCB) stars, extreme helium B stars, helium-rich subdwarf O stars, and the O(He) central stars. They all generally have helium-dominated atmospheres, in contrast to [WC] and PG1159 stars, which usually have high carbon abundances. These helium-dominated subtypes might form a distinct post-AGB evolutionary channel being caused by a stellar merging event. Because the origin of their abundance patterns is unclear, they are (at the moment) not useful for probing AGB evolution. Therefore, we discuss these subtypes for completeness only (§ 2.3), to order the zoo of H-deficient post-AGB stars.

Table 1 gives an overview of typical abundance patterns found among all the spectral subclasses discussed. The [WC] stars are subdivided into late- and early-type stars, [WCL] and

TABLE 1
ELEMENTAL ABUNDANCES (MASS FRACTIONS) IN REPRESENTATIVE HYDROGEN-DEFICIENT POST-AGB STARS OF DIFFERENT SPECTRAL CLASSES

Star	$T_{\rm eff}$ (K)	log g (cgs)	H	He	C	N	O	F	Ne	Si	S	Fe	Note	Reference
[WCL]														
IRAS 21282	28,000	3.2	0.10	0.43	0.46	<0.005	0.01	…	…	<0.001	…	…	H present	2
PM 1-188	35,000	3.7	0.01	0.39	0.47	0.01	0.07	…	0.03	0.025	…	…	N present, Si high	2
He 2-459	77,000	4.4	<0.02	0.40	0.50	…	0.10	…	…	…	…	…	Typical He/C/O	2
[WCE]														
NGC 1501	134,000	6.0	…	0.50	0.35	…	0.15	…	…	…	…	…	Typical He/C/O	1
Sanduleak 3	140,000	6.0	…	0.62	0.26	0.005	0.12	…	…	…	…	…	N present	3
[WC]–PG1159														
Abell 78	115,000	5.5	…	0.33	0.50	0.02	0.15	1.0×10^{-5}	…	…	…	<0.0001	Fe deficient	4, 10, 18
PG1159														
HS 1517+7403	110,000	7.0	…	0.85	0.13	$<3 \times 10^{-5}$	0.02	…	…	…	…	…	C, O low	5
HS 2324+3944	130,000	6.2	0.17	0.35	0.42	<0.0003[a]	0.06	…	…	…	…	…	H present	11
PG 1159−035	140,000	7.0	<0.02	0.33	0.48	0.001	0.17	3.2×10^{-6}	0.02	0.00036	0.00001	<0.0003	Typical He/C/O	6, 7, 9, 10, 19
PG 1144+005	150,000	6.5	…	0.38	0.57	0.015	0.016	1.0×10^{-5}	0.02	…	…	…	O low	8, 9, 10
RCB														
RY Sgr	7250	0.7	6×10^{-6}	0.98	0.007	0.003	0.0009	…	…	0.00040	0.00045	0.00020	…	12
Extreme He-B Stars														
BD +10 2179	16,900	2.5	1×10^{-4}	0.98	0.02	0.0008	0.0004	…	…	0.00013	0.00007	0.00063	…	13
He-sdO														
BD +37 442	60,000	4.0	<0.001	0.97	0.025	0.003	…	…	…	0.00079	…	…	…	14
KS 292	75,000	5.5	0.32	0.65	0.023	0.013	…	…	…	…	…	…	…	15
O(He)														
K1-27	105,000	6.5	<0.05	0.98	<0.015	0.017	…	…	…	…	…	…	N present	16
LoTr 4	120,000	5.5	0.11	0.89	<0.010	0.003	<0.03	…	…	…	…	…	H, N present	16
HS 1522+6615	140,000	5.5	0.02	0.97	0.01	…	…	…	…	…	…	…	H, C present	16
The Sun	…	…	0.73	0.25	0.0029	0.00089	0.0079	5.0×10^{-7}	0.0018	0.00072	0.00050	0.0013	…	17

NOTE.—We discuss two possible evolutionary sequences: (1) [WCL] → [WCE] → [WC]–PG1159 → PG1159, and (2) RCB → extreme He-B stars → He-sdO → O(He).

[a] Uncertain.

REFERENCES.—(1) Koesterke & Hamann 1997b; (2) Leuenhagen & Hamann 1998; (3) Koesterke & Hamann 1997a; (4) Werner & Koesterke 1992; (5) Dreizler & Heber 1998; (6) Werner et al. 1991; (7) Werner 1996; (8) Werner & Heber 1991; (9) Werner et al. 2004c; (10) Werner et al. 2005; (11) Dreizler 1998; (12) Asplund et al. 2000; (13) Pandey et al. 2006; (14) Bauer & Husfeld 1995; (15) Rauch et al. 1991; (16) Rauch et al. 1998; (17) Grevesse & Sauval 2001; (18) Werner et al. 2003; (19) Jahn 2005.

[WCE]. In addition, a [WC]–PG1159 transition type has been introduced, denoting objects with a mixed emission- and absorption-line spectrum.

2.1. PG1159 Stars

2.1.1. Spectral Classification

The optical spectra of PG1159 stars are characterized by weak and broad absorption lines of He II and C IV, sometimes with central emission reversals. The hottest objects also display O VI and Ne VII lines. Three spectral subclasses have been introduced that allow a coarse characterization of each star. According to the appearance of particular line features, the subtypes "A" (absorption lines), "E" (emission lines), and "lgE" (low gravity with emission lines) were defined (Werner 1992).

2.1.2. General Characteristics: Temperature, Gravity, and **He/C/O** *Abundances and Mass-Loss Rates*

Quantitative spectral analyses first became feasible with the construction of line-blanketed non-LTE model atmospheres that accounted for peculiar chemical compositions (Werner et al. 1991). At that time, only a handful of PG1159 stars had been identified. Today, 40 such stars are known. Most of them were found by systematic spectroscopic observations of the central stars of old, evolved planetary nebulae (Napiwotzki & Schönberner 1995), as well as follow-up spectroscopy of faint blue stars from various optical sky surveys (the Palomar-Green survey, Montreal-Cambridge-Tololo Survey, Hamburg-Schmidt and Hamburg/ESO Surveys, and Sloan Digital Sky Survey) and soft X-ray sources detected in the *ROSAT* All-Sky Survey.

TABLE 2
KNOWN PG1159 STARS AND THE RESULTS OF SPECTROSCOPIC ANALYSES

Star	$T_{\rm eff}$ (10^3 K)	log g (cgs)	C/He[a]	O/He	Mass ($M_\odot$)	Variable	PN	Reference[b]	Remark[c]
H1504+65	200	8.0	>50	>50	0.89	No	No	1	He deficient
RX J0122.9−7521	180	7.5	0.3	0.17	0.72	No	No	2	
RX J2117.1+3412	170	6.0	1.4	0.16	0.70	Yes	Yes	3	
HE 1429−1209	160	6.0	1.4	0.16	0.67	Yes	No	4	
PG 1520+525	150	7.5	0.9	0.4	0.67	No	Yes	3	
PG 1144+005	150	6.5	1.5	0.05	0.60	No	No	3	
Jn 1	150	6.5	1.5	0.8	0.60	No	Yes	5	
NGC 246	150	5.7	0.5	0.1	0.72	Yes	Yes	3	
PG 1159−035	140	7.0	1.5	0.5	0.60	Yes	No	3	
NGC 650	140	7.0	?	?	0.60	No	Yes	6	:
Abell 21 (=Ym 29)	140	6.5	1.5	0.5	0.58	No	Yes	2	:
K1-16	140	6.4	1.5	0.5	0.58	Yes	Yes	3	:
Longmore 3	140	6.3	1.4	0.16	0.59	No	Yes	2	:
PG 1151−029	140	6.0	1.5	0.5	0.60	No	No	2	:
VV 47	130	7.0	1.5	0.4	0.59	No	Yes	5	:
HS 2324+3944	130	6.2	1.2	0.16	0.58	Yes	No	11	:, hybrid
Longmore 4	120	5.5	0.9	0.2	0.65	Yes	Yes	3	
SDSS J001651.42−011329.3	120	5.5	0.3	0.16	0.65	…	No	7	
SDSS J102327.41+535258.7	110	7.6	0.33	?	0.65	No	No	7	
PG 1424+535	110	7.0	0.9	0.12	0.57	No	No	3	
HS 1517+7403	110	7.0	0.15	0.02	0.57	No	No	9	
Abell 43	110	5.7	1.2	0.16	0.59	Yes	Yes	11	:, hybrid
NGC 7094	110	5.7	1.2	0.16	0.59	No	Yes	11	:, hybrid
SDSS J075540.94+400918.0	100	7.6	0.09	?	0.62	…	No	7	
SDSS J144734.12+572053.1	100	7.6	0.15	?	0.62	No	No	7	
SDSS J134341.88+670154.5	100	7.6	0.15	?	0.62	No	No	7	
SDSS J093546.53+110529.0	100	7.6	0.15	?	0.62	No	No	7	
SDSS J121523.09+120300.8	100	7.6	0.15	?	0.62	…	No	7	
HS 0444+0453	100	7.5	?	?	0.59	…	No	8	:
IW 1	100	7.0	?	?	0.56	No	Yes	6	:
Sh 2-68	96	6.8	?	?	0.55	…	Yes	10	:, hybrid
PG 2131+066	95	7.5	0.9	0.4	0.58	Yes	No	9	
MCT 0130−1937	90	7.5	0.3	0.04	0.60	No	No	2	
SDSS J034917.41−005919.3	90	7.5	0.9	?	0.60	…	No	7	
PG 1707+427	85	7.5	0.9	0.4	0.59	Yes	No	3	
PG 0122+200	80	7.5	0.9	0.4	0.58	Yes	No	9	
HS 0704+6153	75	7.0	0.3	0.12	0.51	…	No	9	
NGC 6852	…	…	…	…	…	…	Yes	6	K1-16 type
NGC 6765	…	…	…	…	…	…	Yes	6	K1-16 type
Sh 2-78	…	…	…	…	…	…	Yes	6	PG 1424+535 type

NOTE.—Objects with detectable residual hydrogen are denoted "hybrid" stars. It is also noted if the star is a pulsating variable object and if it has a planetary nebula. No spectroscopic analysis of the last three stars was performed. [WC]–PG1159 transition-type objects such as Abell 78 and Abell 30 are not listed.

[a] Abundance ratios by mass.

[b] Refers to the most recent spectroscopic work.

[c] Colons denote uncertain preliminary results of spectroscopic analyses.

REFERENCES.—(1) Werner et al. 2004a; (2) Werner et al. 2004c; (3) Werner et al. 2005; (4) Werner et al. 2004b; (5) Rauch & Werner 1995; (6) Napiwotzki & Schönberner 1995; (7) Hügelmeyer et al. 2006; (8) Dreizler et al. 1995; (9) Dreizler & Heber 1998; (10) Napiwotzki 1999; (11) Dreizler 1998.

In Table 2 we give a complete list of all known PG1159 stars, and their location in the $T_{\rm eff}$– log g diagram is shown in Figure 2. It can be seen that they span a wide range in temperature and gravity. They represent stars in their hottest phase of post-AGB evolution. Some of them (those with $\log g \lesssim 6.5$) are still helium-shell burners (located before the "knee" in their evolutionary track), while the majority have already entered the WD cooling sequence.

Estimates for mass and luminosity can be obtained by comparison with theoretical evolutionary tracks. The mean mass of PG1159 stars is 0.62 $M_\odot$, using the older models of H-rich central stars (Fig. 2, *solid and dashed lines*). However, the H-deficient 0.604 $M_\odot$ track (Fig. 2, *dash-dotted line*) is systematically hotter than the older tracks and indicates that in fact the central stars are on average somewhat less massive than that. It is important to note that the higher temperature of the

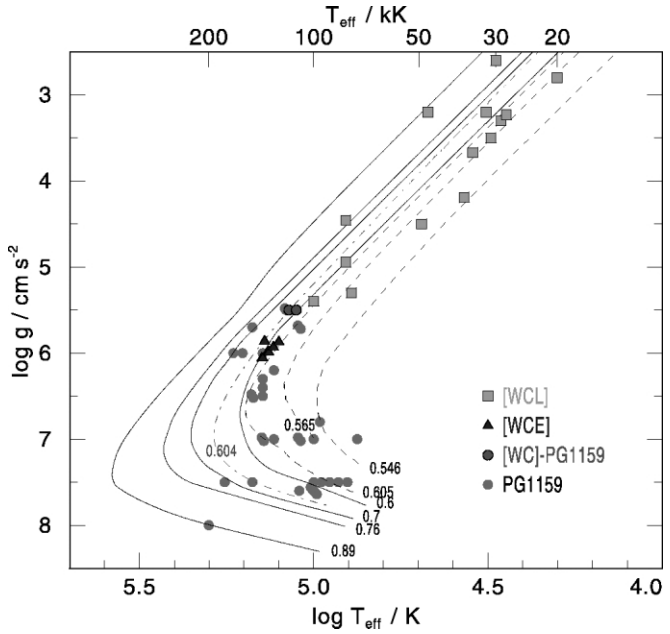

FIG. 2.—Hot hydrogen-deficient post-AGB stars in the g-$T_{\rm eff}$ plane. We identify Wolf-Rayet central stars of early and late type ([WCE] and [WCL]) from Hamann (1997), PG1159 stars (from Table 2), as well as two [WC]–PG1159 transition objects (Abell 30 and Abell 78). The $T_{\rm eff}$ for the [WC] stars is related to the stellar radius at $\tau_{\rm Ross} = 20$. Evolutionary tracks are from Schönberner (1983) and Blöcker (1995; *dashed lines*), Wood & Faulkner (1986), and Herwig (2003; *dash-dotted line*). Labels indicate mass in $M_{\odot}$. The latter 0.604 $M_{\odot}$ track is the final CSPN track following VLTP evolution and therefore has a H-deficient composition. However, the difference between the tracks is mainly due to the different AGB progenitor evolution. [*See the electronic edition of the PASP for a color version of this figure*.]

new tracks is not the result of being H deficient. Instead, the reason is the more realistic AGB progenitor evolution that now includes the third dredge-up after most of the AGB thermal pulses. This leads to a higher luminosity for a given core mass, and during the post-AGB evolution, to higher temperature (§ 3.2.4).

Optical spectra are dominated by numerous He II and C IV lines, from which the He/C ratio can be derived. In addition, only the hottest objects ($T_{\rm eff} \gtrsim 120{,}000$ K) exhibit oxygen lines (O VI and, sometimes, very weak O V), so the O abundance in cooler stars cannot be determined unless UV spectra are available. Similarly, only the hottest objects display optical neon lines (Ne VII), and only UV spectra allow access to the neon abundance in the case of cooler objects. Hydrogen poses a special problem, because all H lines are blended with He II lines. In medium-resolution (≈1 Å) optical spectra, hydrogen is only detectable if its abundance is higher than about 0.1 (all abundances in this paper are given in mass fractions). With high-resolution spectra, which are difficult to obtain because of the faintness of most objects, this limit can be pushed down to about 0.02. For PG1159 stars within a PN, the situation is even more difficult, because of nebular Balmer emission lines.

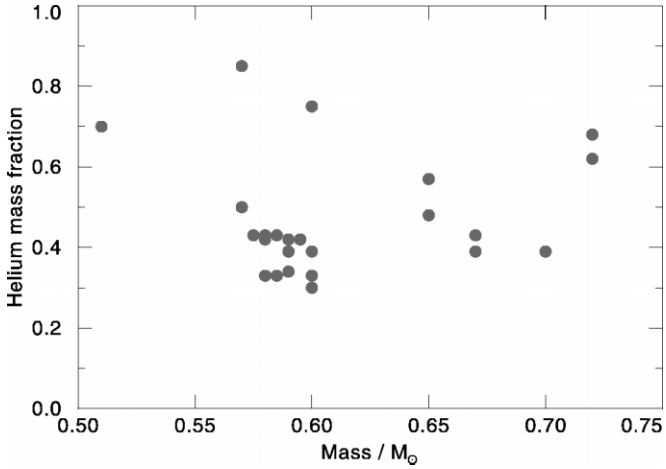

FIG. 3.—Helium mass fraction in PG1159 stars as a function of stellar mass. [*See the electronic edition of the PASP for a color version of this figure*.]

The He, C, and O abundances show strong variations from star to star; however, a word of caution is also appropriate here. The quality of the abundance determination is also very different from star to star. For some objects, only relatively poor optical spectra were analyzed, while others were scrutinized with great care using high signal-to-noise ratio (S/N), high-resolution optical *and* UV/far-UV (FUV) data. Nevertheless, we think that the abundance scatter is real. The prototype PG 1159−035 displays what could be called a "mean" abundance pattern: He/C/O = 0.33/0.50/0.17. For instance, an extreme case with low C and O abundances is HS 1517+7403, which has He/C/O = 0.85/0.13/0.02. Taking all analyses into account, the range of mass fractions for these elements is approximately He = 0.30–0.85, C = 0.15–0.60, and O = 0.02–0.20 (excluding the peculiar object H1504+65; see § 2.1.11). There is a strong preference for a helium abundance in the range 0.3–0.5, independent of the stellar mass (Fig. 3). Only a minority of stars has a higher He abundance, namely in the range 0.6–0.8. There is a tendency for high O abundances only to be found in objects with high C abundances (Fig. 4).

Some remarks on the possible analysis errors are necessary. As just pointed out, the observational data are of rather diverse quality, but in general the following estimates hold. The temperature determination is accurate to 10%–15%. The surface gravity is uncertain within 0.5 dex. Elemental abundances should be accurate within a factor of 2. The main problem arises from uncertainties in line-broadening theory, which directly affects the gravity determination and the abundance analysis of He, C, and O.

2.1.3. Objects with Residual Hydrogen: Hybrid PG1159 Stars

We already mentioned that hydrogen is difficult to detect. However, four objects clearly show Balmer lines, and they are

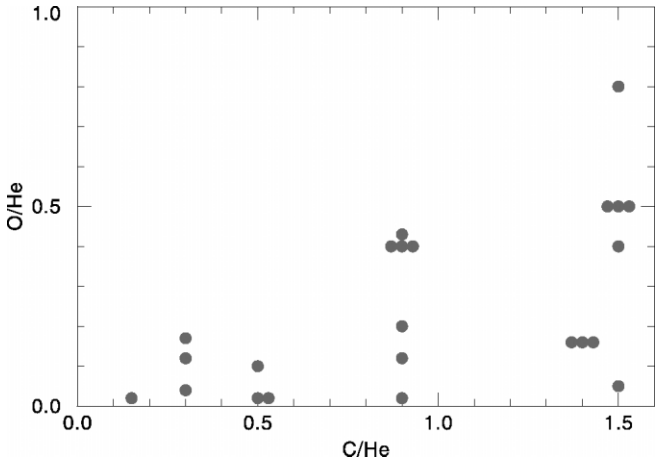

FIG. 4.—Carbon and oxygen abundance ratios relative to helium (by mass) in PG1159 stars. [*See the electronic edition of the PASP for a color version of this figure.*]

called hybrid PG1159 stars. The deduced H abundance is quite high, H = 0.17 (Table 1; Dreizler 1998). It is worthwhile to note for discussion of their evolution that nitrogen is seen in the optical spectra of some of these stars, but quantitative analyses are still lacking. The hybrid star NGC 7094 shows Ne and F enhancements, as do many PG1159 stars (see below). Therefore, one can conclude that aside from the presence of H, the elemental abundance pattern of the hybrid PG1159 stars seems to resemble that of many other PG1159 stars. However, not all the hybrids have been analyzed appropriately yet, although good UV and optical spectra are available.

2.1.4. Nitrogen and Pulsation Instability

Some PG1159 stars do show nitrogen lines while others with similar temperature and gravity do not. These are N V lines in the optical wavelength range and the resonance-line doublet in the UV at 1239/1243 Å. The derived N abundance is of the order 0.01 (Werner & Heber 1991; Dreizler & Heber 1998). The presence of N shows no clear correlation to the relative abundances of the main atmospheric constituents (He, C, and O). However, a remarkable correlation between the presence of N and the pulsational instability of PG1159 stars has been found: all four pulsating objects in a sample of nine examined PG1159 stars show nitrogen (Dreizler & Heber 1998). Among these objects is the prototype PG 1159−035, for which we have recently taken a high-resolution *Hubble Space Telescope* (*HST*) Space Telescope Imaging Spectrograph (STIS) spectrum, allowing us to separate the interstellar and photospheric components of the N V resonance doublet. As a consequence, we find that the N abundance is distinctly lower, namely 0.001 (E. Reiff et al. 2006, in preparation; Jahn 2005; Reiff et al. 2005), which weakens the nitrogen/pulsation correlation. In any case, such a correlation is difficult to explain with current stellar pulsation models (e.g., Quirion et al. 2004). Due to its low abundance, nitrogen cannot affect pulsational properties, but it has been speculated that N is a marker for different evolutionary histories leading to different He/C/O abundances in the pulsation-driving regions. More about PG1159 pulsators follows in § 2.1.13.

2.1.5. Neon

Neon has been detected in 10 PG1159 stars by the identification of Ne VII lines in optical and FUV spectra (Werner & Rauch 1994; Werner et al. 2004c). The derived abundances are of the order 0.02; i.e., roughly 10 times solar. Only the hottest and most luminous objects are able to ionize neon strongly enough to show these lines. Unfortunately, no lines from lower ionization stages are observed, so the neon abundance in cooler PG1159 stars remains unknown. The strongest Ne VII line is found in *Far Ultraviolet Spectroscopic Explorer* (*FUSE*) spectra, located at 973 Å. The absorption-line core almost reaches zero intensity in some objects. In the most luminous objects (e.g., K1-16), this line displays a powerful P Cygni profile (Herald et al. 2005).

2.1.6. Fluorine

Lines from F V and F VI have been discovered in *FUSE* spectra of several PG1159 stars (Werner et al. 2005). The derived abundances show a surprisingly strong variation from star to star, ranging between solar and 250 times solar. Correlations between the fluorine and other elemental abundances are not obvious. We have speculated that the variety of F abundances is a consequence of the stellar mass, which according to Lugaro et al. (2004), strongly affects the production of fluorine.

2.1.7. Other Light Metals: Silicon, Phosphorus, and Sulfur

Lines from silicon, phosphorus, and sulfur have been discovered in *FUSE* spectra of several PG1159 stars. Analyses are currently being performed, so we can only report preliminary results (E. Reiff et al. 2006, in preparation; Jahn 2005; Reiff et al. 2005).

The silicon abundance in PG1159 stars is of interest because a strong overabundance (up to Si = 0.03; i.e., 40 times solar) has been found in a handful of [WCL] stars (Leuenhagen & Hamann 1998). The photospheric component of the Si IV λλ1394, 1402 resonance doublet has been identified in the aforementioned *HST* STIS high-resolution spectrum of the prototype. Our best line fit is obtained with Si = 0.5 solar, which indicates no significant deviation from the solar abundance within error limits. Another silicon line pair, Si IV λλ1122, 1128, can be identified in relatively cool objects only. For PG 1424+535 we find a solar silicon abundance from these lines and an upper limit of 0.1 times solar for PG 1520+525.

Phosphorus was discovered in a number of PG1159 stars

by the identification of the P v resonance doublet at 1118 and 1128 Å. First results for two objects indicate a roughly solar abundance.

The most prominent sulfur feature is the S vi λλ933, 945 resonance doublet. It was first detected in K1-16, and a solar S abundance was derived (Miksa et al. 2002). It is also visible in other PG1159 stars. In the prototype star and two other objects, we find a surprisingly strong S depletion (less than 1/10 solar).

2.1.8. Iron Deficiency

Model spectra for PG1159 stars predict detectable lines from Fe vi and Fe vii in the UV for objects that are not too hot ($T_{\rm eff} \leq 140{,}000$ K); otherwise iron is ionized to even higher stages that have lines only in the EUV range, beyond the Lyman edge. But iron lines are narrow and require high-resolution (≈0.1 Å), high-S/N spectra for quantitative analysis. Up to now, iron has not been detected in *any* PG1159 star. In most cases, a solar Fe abundance cannot be excluded, because the data quality does not allow more stringent conclusions. For two PG1159 stars, however, it has been shown that the lack of iron lines means that the iron abundance is subsolar by at least 1 dex (K1-16 and NGC 7094; Miksa et al. 2002). A similar result was obtained for the [WC]–PG1159 transition object Abell 78 (Werner et al. 2003) and several [WC] stars (see below). The prototype, PG 1159−035, is subsolar in Fe by at least a factor of 5 (Jahn 2005). The suggestion of Herwig et al. (2003b) that iron has been transformed into heavier elements is discussed below. Our search for lines from elements heavier than Fe has so far been unsuccessful.

2.1.9. Unidentified Lines

About two dozen absorption lines in the 1000–1700 Å region of PG1159 stellar spectra taken with *FUSE*, *HST*, and *IUE* (the *International Ultraviolet Explorer*) remain unidentified. Most of them are commonly seen in at least two objects, and many are quite prominent. For example, one of the strongest unidentified absorption lines in the UV spectrum of the prototype, and also of other PG1159 stars, is located at 1270.2 Å. It always appears together with a small number of weaker absorption lines in the 1264–1270 Å range. It could be a hitherto unidentified neon or magnesium multiplet.

In addition, a number of weak lines in high-quality optical spectra also remain unidentified. We have recently identified one of these features as a Ne vii multiplet, whose wavelength was only inaccurately known before (Werner et al. 2004c).

We are confident that all the unidentified lines do not stem from C or O. On the other hand, it is obvious that line lists from other highly ionized metals are rather incomplete, inaccurate, or even nonexistent. Some of the unidentified lines might stem from other light metals (Mg and Al) or even from heavy metals beyond the iron group (e.g., *s*-process–enhanced elements). Every effort should be made to identify these lines. New species could be found, and their abundances checked against evolutionary models.

2.1.10. Mass Loss and Occurrence of Ultra–High-Ionization Lines

PG1159 stars do not exhibit wind features in their optical spectra. However, UV spectroscopy reveals that many of the low-gravity central stars display strong P Cygni profiles; e.g., the resonance lines from C iv and O vi, and subordinate lines from He ii, O v, and Ne vii. Mass-loss rates in the range $\log(\dot{M}/[M_\odot\ \mathrm{yr}^{-1}]) = -8.3, \ldots, -6.9$ were derived (Koesterke & Werner 1998; Koesterke et al. 1998; Herald et al. 2005), and it appears that they are in accordance with predictions from radiation driven–wind theory.

The central star of Longmore 4 showed a remarkable event in which its spectral type turned from PG1159 to [WCE] and back again to PG1159, most probably due to a transient but significant increase in the mass-loss rate (Werner et al. 1992). The reason is unknown but might be connected to the fact that the star is a pulsator. This phenomenon has not been witnessed since, either in Longmore 4 or any other PG1159 star. The outburst phenomenon observed in the [WR] central star of the LMC planetary nebula N66 is probably the consequence of mass transfer within a close binary system (see § 2.2.4).

The most luminous PG1159 stars display ultra–high-ionization *emission* lines, the most prominent of which is O viii λ6068 (e.g., Werner et al. 1994). This phenomenon is also seen in [WCE] stars and in [WC]–PG1159 transition objects, as well as in the hottest known DO white dwarf (KPD 0005+5106). It is clear that the photospheric temperatures are not high enough to produce these lines, and it is possible that they arise from shock-heated regions in the stellar wind.

A large fraction of all DO white dwarfs show such ultra–high-ionization lines in *absorption* (e.g., C vi, N vii, O viii, and Ne x; Werner et al. 1995). This remarkable and still unexplained phenomenon was recently discovered in a new PG1159 star (Hügelmeyer et al. 2006). In addition, the usual photospheric absorption lines (He ii and C iv) are much stronger than predicted from any model, and this behavior is also shared with that of the respective DO white dwarfs.

We remark that, even more strangely, too-deep photospheric He ii absorption lines are exhibited by some DO white dwarfs that do *not* show ultrahigh-ionization absorption lines at the same time (e.g., Werner et al. 2004b). A similar PG1159-type counterpart has also been discovered (Nagel et al. 2006).

2.1.11. Peculiar: H1504+65

H1504+65 displays an optical spectrum that is at first sight rather similar to other hot, high-gravity PG1159 stars. However, it has been shown that this object is helium deficient and that its atmosphere is mainly composed of C and O. It probably

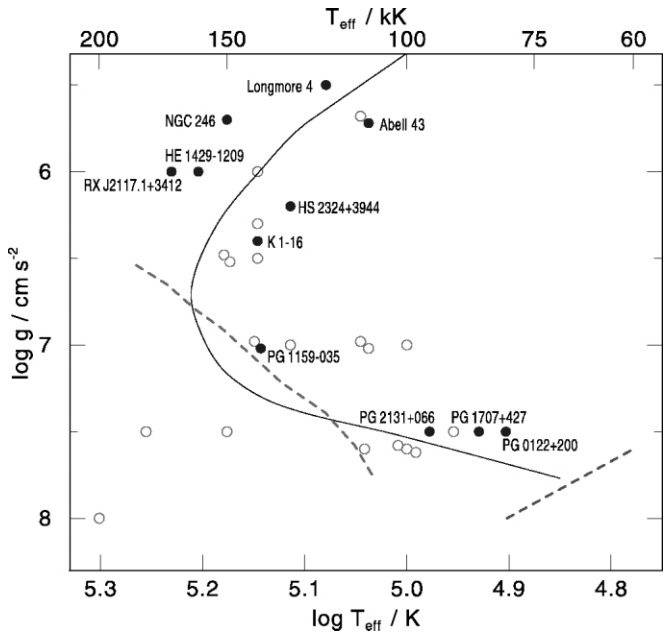

FIG. 5.—Pulsating PG1159 stars (*filled circles with labels*) and the nonpulsators. The dashed lines show theoretical blue and red edges of the instability strip, from Gautschy et al. (2005) and Quirion et al. (2004), respectively. See text for a discussion of these edges and the coexistence of nonpulsators in the strip (§ 2.1.13). Also shown is the 0.6 $M_{\odot}$ post-AGB track from Fig. 2. [*See the electronic edition of the PASP for a color version of this figure*.]

has an evolutionary history that is different from all the other PG1159 stars; hence, we refrain from further discussion of this interesting peculiar object (for details, see Werner et al. 2004a).

2.1.12. Descendants: DA and Non-DA White Dwarfs

The coolest high-gravity PG1159 star has $T_{\rm eff} = 75{,}000$ K, and the hottest white dwarfs have $T_{\rm eff} \approx 120{,}000$ K. In this temperature range, the PG1159 stars must be turned into DA or non-DA white dwarfs by gravitational settling, depending on the presence of residual hydrogen in the PG1159 stellar envelope. It is tempting to assume that the majority of the PG1159 stars will become DO and then DB and DQ white dwarfs, but it is unknown to what extent this is true. Clearly, the hybrid PG1159 stars will become DA white dwarfs, but this could in principle also hold for all other PG1159 stars, because a H abundance as high as 0.01 cannot be excluded by spectroscopic means. Depending on the amount of residual H in the PG1159 envelope, DA white dwarfs with different hydrogen-layer mass will emerge. It can be speculated that the ZZ Ceti stars (DA pulsators) for which thin H envelopes were inferred are descendants of PG1159 stars (Althaus et al. 2005a).

2.1.13. Results from Asteroseismology

Some of the PG1159 stars are nonradial *g*-mode pulsators (see Table 2), and they define the GW Virginis (=PG 1159−035) instability strip in the Hertzsprung-Russell diagram (HRD; Fig. 5). These variables are among the best studied by asteroseismological analysis. Such investigations of the interior of PG1159 stars hold important clues to their origin.

TABLE 3
RESULTS FROM ASTEROSEISMOLOGY OF PG1159 STARS AND THE [WC4] CENTRAL STAR OF NGC 1501

Star	$M_{\rm spec}$	$M_{\rm puls}$	$M_{\rm env}$	$P_{\rm rot}$	Reference
PG 2131+066	0.58	0.61	0.006	0.21	1
PG 0122+200	0.58	0.59	...	1.66	2
RX J2117.1+3412	0.70	0.56	0.045	1.16	3
PG 1159−035	0.60	0.59	0.004	1.38	4
PG 1707+427	0.59	0.57	...	...	5
NGC 1501	...	0.55	...	1.17	6

NOTE.—We compare the stellar mass derived by spectroscopic means $M_{\rm spec}$ (from Table 2) with the pulsational mass $M_{\rm puls}$. Other columns list envelope mass $M_{\rm env}$ (all masses in solar units) and rotation period $P_{\rm rot}$ in days.

REFERENCES.—(1) Kawaler et al. 1995; (2) Fu & Vauclair 2006; (3) Vauclair et al. 2002; (4) Kawaler & Bradley 1994; (5) Kawaler et al. 2004; (6) Bond et al. 1996.

In Table 3 we summarize the results from asteroseismology of five PG1159 stars, plus one [WCE] central star. The agreement between pulsational and spectroscopic mass determinations is very good (within 5%), except for RX J2117.1+3412, for which the difference is of the order 20%. This is significant because in order to shift its position in the $\log g - \log T_{\rm eff}$ diagram onto the $M_{\rm puls} = 0.56\ M_{\odot}$ track, $T_{\rm eff}$ would need to be decreased from 170,000 to <120,000 K, which is clearly ruled out by detailed optical and UV/FUV spectroscopy. The mass discrepancy is possibly due to inadequate pulsation models, a weakness in their asteroseismic analyses that was pointed out by Vauclair et al. (2002).

Of considerable interest for comparisons with evolutionary calculations is the analysis of the mode-trapping features in the period spacings, which allows us to investigate the stellar interior structure. Table 3 lists the results obtained for the stellar envelope mass $M_{\rm env}$; i.e., the mass above the chemical discontinuity between the He-rich envelope and the C-O core. These envelope masses are much smaller than the intershell region remaining on top of the C-O core ($M = 2 \times 10^{-2}\ M_{\odot}$) immediately after a (very) late thermal pulse. The observational mass-loss determination for FG Sge by Gehrz et al. (2005) shows that born-again stars have high mass-loss rates over prolonged periods of time (see § 2.4). These may remove enough mass to indeed identify the envelope mass from pulsation analyses with the mass between the He-free core and the surface. Note, however, that recent investigations involving complete evolutionary models have come to the conclusion that the mode-trapping features could result from structures in the C-O core (Córsico & Althaus 2005).

Recent theoretical pulsation-driving modeling could clarify important problems. Early stability calculations (e.g., Starrfield et al. 1983) suggested that the C-O κ-mechanism in PG1159 stars

is suffering from the so-called H- and He-poisoning phenomenon. Accordingly, the He abundance in the photospheres, and particularly the H abundance in the hybrid PG1159 stars, is too high to drive pulsations in the subphotospheric layers; hence, abundance gradients had to be invoked. However, it is difficult to explain how such an abundance gradient could be maintained. The κ-mechanism operates at depths where $T \approx 10^6$ K, which lies in the outer $\approx 10^{-8} M_\star$ mass fraction of the star (e.g., Quirion et al. 2004). In the case of RX J2117.1+3412, for instance, the observed mass-loss rate of $\log (\dot{M}/[M_\odot\ \mathrm{yr}^{-1}]) = -7.4$ (Koesterke & Werner 1998) implies that the material in the driving region is appearing on the surface and is renewed on a very short timescale, namely 3 months. New pulsation modeling with improved opacity tables has shown that this poisoning problem is not so severe, and hence no abundance gradients need to be invoked (Saio 1996; Gautschy 1997; Gautschy et al. 2005; Quirion et al. 2004). They can even explain the presence of pulsations in the H-rich hybrid PG1159 stars (Quirion et al. 2005a). However, these results are still at odds with similar calculations performed by others (Cox 2003).

The coexistence of pulsators and nonpulsators in the instability strip can be explained in terms of differences in the chemical surface composition. The red edge of the strip is essentially identical to the location of the coolest high-gravity PG1159 stars. Gravitational diffusion of C and O out of the remaining He envelope removes the driving agents and turns the PG1159 star into a DO white dwarf (Quirion et al. 2005b). There is no sharp blue edge of the strip, as its position is different for each star, depending on its chemical composition. Asteroseismic analyses of DB white dwarfs confirm the diffusion scenario and the PG1159–DO–DB evolutionary link (Metcalfe et al. 2005).

2.2. [WC] Central Stars

[WC] central stars exhibit spectra that are very similar to their massive counterparts. As a consequence of the higher mass-loss rates [$\log (\dot{M}/[M_\odot\ \mathrm{yr}^{-1}]) = -7.0, \ldots, -4.9$; Koesterke 2001] compared to PG1159 stars, they show essentially pure emission-line spectra, mainly presenting broad and bright lines of He, C, and O.

Recent summaries of [WC] identifications and spectral analyses can be found in Acker & Neiner (2003) and Hamann (2003), respectively.

2.2.1. Abundances in [WC] Stars Compared to PG1159 Stars

The [WC] stars are divided into two subgroups, namely late- and early-type objects: [WCL] and [WCE]. From their location in the $\log g$– $\log T_{\rm eff}$ diagram (Fig. 2), it is suggestive that they form an evolutionary sequence, but this is at odds with the current state of quantitative spectral analyses. The mean carbon abundance in [WCL] stars is 0.50, while it is lower by about a factor of 2 in the [WCE]s (Koesterke 2001). In recent reanalyses with new models, this difference does not disappear (Hamann et al. 2005). It is conceivable that systematic errors occur because the abundance analyses rely on different spectral lines in [WCL]s and [WCE]s.

Aside from this discrepancy, it seems obvious that the PG1159 stars are the progeny of [WC] stars, because they can accommodate the variety of He/C abundance ratios observed in the [WC]s. To corroborate this evolutionary link, it is useful to compare other elemental abundances. We refer to work already quoted in this section and to Leuenhagen & Hamann (1998).

1. *Hydrogen*.—In three [WCL] stars H was detected, and the abundances range between 0.1 and 0.01, although it has been questioned whether the Balmer lines are of photospheric origin (De Marco & Barlow 2001). No H was detected in [WCE] stars, but no strict upper limits can be given ($\mathrm{H} \lesssim 0.1$). This is in line with upper limits of about 0.1 for the H abundance in PG1159 stars and the H abundance of 0.17 in the hybrid PG1159 stars.

2. *Nitrogen*.—Some [WCL] stars exhibit N lines, and abundances of the order 0.01 were found. In addition, some [WCE]s show N lines, and the derived abundances are just slightly lower, namely 0.003–0.005. These abundances are very similar to those determined for objects in the PG1159 group.

3. *Oxygen*.—The range of O abundances observed in [WC]s is very similar to that of the PG1159 stars.

4. *Neon*.—Ne I lines were detected in four [WCL] stars, and abundances of the order 0.03 were derived. Again, this is very similar to the PG1159 group.

5. *Silicon*.—As mentioned above (§ 2.1.7), strong Si overabundances in some [WCL] stars were found, which is at odds with the approximately solar Si abundance we find in the PG1159 prototype. More analyses are needed to see if there exists a large abundance scatter within the [WCE] or PG1159 stars.

6. *Iron*.—As in the case of the PG1159 stars, the Fe abundance in [WC] stars has been examined in a few cases only. An iron deficiency has been found that is in qualitative agreement with PG1159 stars. Gräfener et al. (2003) report a low Fe abundance in SMP 61, a [WCE] star in the LMC. Its abundance is at least 0.7 dex below the LMC metallicity. Crowther et al. (1998) find evidence for an underabundance of 0.3–0.7 dex in the Galactic [WCL] stars NGC 40 and BD +30 3639.

2.2.2. [WC]–PG1159 Transition Objects and Weak Emission Line Stars (WELSs)

The [WC]–PG1159 class comprises stars that show spectral characteristics of both PG1159 and [WC] stars, namely mixed absorption- and emission-line spectra. Only two objects can be safely assigned to this group (Abell 30 and Abell 78). They

have He/C/N/O abundances similar to PG1159 and [WC] stars (Werner & Koesterke 1992).

It must be emphasized that the class of so-called weak emission line stars (WELSs), which comprises dozens of central stars (e.g., Tylenda et al. 1993), is *not* identical to the [WC]–PG1159 class. The WELSs are poorly studied quantitatively, and some of them are clearly "usual" hydrogen-rich post-AGB stars (Méndez 1991; Fogel et al. 2003).

2.2.3. WO and O VI *Classifications*

The term "O VI sequence" was coined by Smith & Aller (1969) to denote central stars with the most highly excited optical stellar spectra. The distinguishing feature of this group is the presence of the O VI λλ3811, 3834 emission doublet. In today's terminology, "O VI stars" is a collective name for the hottest [WCE] and PG1159 stars and the [WC]–PG1159 transition objects, all of which show O VI emission lines.

The WO class (O for oxygen) was first introduced by Barlow & Hummer (1982) for Wolf-Rayet (WR) stars with the highest excitation spectra. It was also introduced in refined classification systems that are applicable to both massive WR stars and WR central stars (Crowther et al. 1998; Acker & Neiner 2003). As in the "O VI sequence," such spectra are exhibited by the hottest objects showing O VI emission lines. In essence, the [WO] classification (with subclasses [WO1] to [WO4]) is used alternatively for the earliest [WCE] subtypes, [WC2] and [WC3].

2.2.4. Are There WN Central Stars?

It is believed that there are two central stars that exhibit a spectrum similar to massive WN stars; i.e., the spectrum is dominated by N instead of C emission lines. For one of these objects (PM 5), it cannot be completely ruled out that it is in fact a massive WN star with a ring nebula (Morgan et al. 2003). The other object is the LMC planetary nebula N66. It is thought that this object is a white dwarf accreting matter from a close companion (Hamann et al. 2003), and hence its surface composition is not the result of single-star evolution.

2.3. He-dominated Post-AGB Objects: RCB, Extreme He-B, He-sdO, and O(He) Stars

There exists a small group of four extremely hot objects ($T_{\rm eff} > 100{,}000$ K) that have almost pure He II absorption-line spectra in the optical. As introduced by Méndez (1991), these stars are classified as O(He). Their atmospheres are indeed helium dominated, and only trace amounts of CNO elements are detected (see also Table 1 for atmospheric parameters; Rauch et al. 1998). In the $\log g - \log T_{\rm eff}$ diagram, they are found among the PG1159 stars. While the born-again evolutionary models can explain the rich diversity of different He/C/O patterns in [WC] and PG1159 stars, they never result in such helium-dominated surface abundances. It is therefore natural to speculate about the existence of a third post-AGB evolutionary sequence and its origin. The O(He) stars could be the long searched-for progeny of the RCB stars, which are relatively cool stars ($T_{\rm eff} < 10{,}000$ K) that also have helium-dominated atmospheres. The so-called extreme He-B stars and the He-sdO (post-AGB) stars are also He dominated and could represent objects in transition phases between RCB and O(He); see Table 1 for the parameters of some representatives.

The evolutionary link between these He-dominated post-AGB objects still needs to be investigated. They are possibly the result of a merging process of two white dwarfs (e.g., Saio & Jeffery 2002), and hence these objects are not of immediate interest to this review.

2.4. Historical (Very) Late He-Shell Flashers

Three stars have been identified as actual born-again stars, mainly through their historical variability. These are FG Sge (Gonzalez et al. 1998), V605 Aql (Clayton & De Marco 1997), and V4334 Sgr (Sakurai's object; Duerbeck & Benetti 1996).

For each of these cases, an important question is whether the born-again evolution is following a very late thermal pulse (VLTP) or just a late thermal pulse (LTP). As we discuss in §§ 3.2.1 and 3.2.3, the difference between the two is that the VLTP happens late during the post-AGB evolution and induces a H-ingestion flash that consumes H in the surface layer by nuclear burning. As recent evolution calculations show (§ 3.2.1), the VLTP born-again star follows a characteristic double loop in the HRD, where the first return to the AGB proceeds quickly, in only a few years, whereas the second return takes much longer, of the order 10^2 yr. The LTP happens earlier, on the horizontal, constant-luminosity part of the post-AGB track, and H deficiency is only the result of dredge-up mixing when the star returns to the AGB. The LTP born-again star follows a single loop on a long timescale, similar to the second return of a VLTP born-again star.

V605 Aql experienced a VLTP in 1917 (Lechner & Kimeswenger 2004). As summarized by Clayton & De Marco (1997 and references therein), it brightened over a period of only 2 yr, followed by three episodes of fading and brightening. Then V605 Aql disappeared, enshrouded in its own dust. In the early 1970s its position was found to coincide with that of the planetary nebula Abell 58. It was later discovered that the PN in fact has a small, high-velocity, H-deficient central knot, while the outer nebula is H normal. Spectra taken in 1986 by Seitter (1987a, 1987b) reveal a broad stellar C IV emission line, indicative of a very hot ($T_{\rm eff} \approx 100{,}000$ K) [WC] central star, implying that V605 Aql had already started to reheat and became a hot H-deficient or H-free central star. A recent model atmosphere analysis of a VLT spectrum taken in 2002 confirms that V605 Aql is now a [WCE] star, having $T_{\rm eff} = 95{,}000$ K (Fedrow et al. 2005).

For FG Sge, it is not so obvious whether it is a LTP or a

VLTP born-again star. Lawlor & MacDonald (2003) proposed that while Sakurai's object and V605 Aql are fast-evolving VLTP first-return born-again objects, FG Sge has also experienced a VLTP but is now on the second long-timescale return. However, as summarized by Gonzalez et al. (1998 and references therein), FG Sge started to brighten in 1894, continuing until the mid-1970s. Since then the brightness has not changed. FG Sge initially (in the 1960s) had solar abundance. Later (in the 1970s), rare earth elements appeared on the surface, and in 1992 the star underwent dramatic photometric variations due to dust condensation. In the 1990s, the carbon and heavy-element abundance further increased, and there is now evidence for H deficiency. The fact that FG Sge had solar abundances 40 yr ago and only rather recently has shown evidence for H deficiency is a clear indication that FG Sge is a LTP star, as pointed out by Gonzalez et al. (1998). A VLTP born-again star during the second loop should already have been extremely H deficient, or likely even H-free, during the entire past observed evolution, which is not the case. We note, however, that it has been questioned whether FG Sge has really become H deficient (Schönberner & Jeffery 2002).

Sakurai's object is the most recently discovered born-again star (Duerbeck et al. 1997, 2000). Its VLTP has been dated semiempirically between 1992 and 1994, and its $T_{\rm eff}$ dropped below 10,000 K in early 1996. At that time the star was already H-poor, and the surface abundance distribution continued to change over a period of 6 months covered by observations by Asplund et al. (1999). While the H abundance was decreasing even further, the already high Li abundance continued to increase. In addition, these observations showed the C, N, and O abundances to be significantly enhanced compared to solar and also showed low $^{12}C/^{13}C$ and Fe/Ni ratios. Since these observations, Sakurai's object has shared the fate of the other born-again objects and faded away behind thick clouds of dust. Recent radio observations show that Sakurai's object has already started to reheat (Hajduk et al. 2005), and it too will eventually become a hot H-free or H-deficient central star.

The observations of born-again stars have revealed important information about the mass loss of these objects. Hajduk et al. (2005) find a mass-loss rate of between 10^{-5} and maybe up to $2 \times 10^{-4}\ M_\odot\ {\rm yr}^{-1}$ for Sakurai's object during the coolest evolution phase. For FG Sge, Gehrz et al. (2005) determined a mass-loss rate of 2.3×10^{-5} to $1.2 \times 10^{-4}\ M_\odot\ {\rm yr}^{-1}$.

3. STELLAR EVOLUTION ORIGIN

The abundance pattern observed in H-deficient bare stellar cores can be understood in terms of the evolutionary origin of these stars. The H- and He-burning shells of AGB stars are the nucleosynthetic origin of the material that is observed at the surface of PG1159 and [WC]-CSPNs. In order to make this connection plausible, we review in this section first those aspects of AGB evolution and nucleosynthesis that are relevant for our purposes, followed by a summary of the current understanding of the born-again evolution that leads to almost complete H depletion. In § 3.3 we describe the surface abundance predictions for H-deficient post-AGB stars.

3.1. AGB Evolution

The basic properties of AGB stars are covered by Iben & Renzini (1983). AGB properties, specifically in view of the post-AGB evolution leading to H-deficient cores, have been summarized by Blöcker (2001), while an extensive review of more recent developments has been provided by Herwig (2005). AGB stars have an electron-degenerate C-O core as a result of core He burning. Their nuclear sources are the He- and H-burning shells that surround the core. Double shell burning on degenerate cores is unstable and is fundamentally similar to the X-ray bursts on the surfaces of neutron stars. AGB stars experience quasi-periodic bursts of the He shell. These He-shell flashes, or thermal pulses, generate a peak luminosity of several times $10^8\ L_\odot$. This large generation of energy causes convective instability of the layer between the He- and H-burning shells. This layer between the shells is the intershell. The convective instability driven by the He-shell flash is the pulse-driven convection zone (PDCZ). The recurrent thermal pulses, as well as the consequences for nucleosynthesis and mixing, are illustrated in Figure 6. This diagram shows the time evolution of the narrow region (in Lagrangian coordinates) from the top of the inert C-O core to the bottom of the envelope convection, which reaches all the way to the surface. The nuclear production in thermally pulsing AGB stars is determined by the interplay of the PDCZ and the envelope convection. This interplay allows the consecutive and alternating exposure of material to He- and H-burning. It can be explained best by following the events of one full pulse cycle, as shown in Figure 6 in detail.

3.1.1. The Thermal Pulse Cycle

The He-burning that provides the energy for the PDCZ is predominantly the 3α reaction, producing ^{12}C from ^4He. In addition, a larger number of additional α-capture reactions are activated. Among these is the $^{22}Ne(\alpha, n)^{25}Mg$ reaction, which releases neutrons and leads to a large neutron flux at the bottom of the PDCZ. We cover the origin of ^{22}Ne in the PDCZ further below. The neutron irradiation has two effects: it leads to the production of many *n*-rich species heavier than iron (the *s*-process elements), and at the same time it reduces the abundance of the seed species of the *s*-process, the most important of which is ^{56}Fe.

The H shell at the bottom of the convective envelope reacts to the perturbation of the He-shell flash in a characteristic way. Due to the expansion and cooling of the layers above the He shell, the H shell is temporarily extinguished. After briefly receding ($0\ {\rm yr} < t < 100\ {\rm yr}$ in Fig. 6), the convective envelope

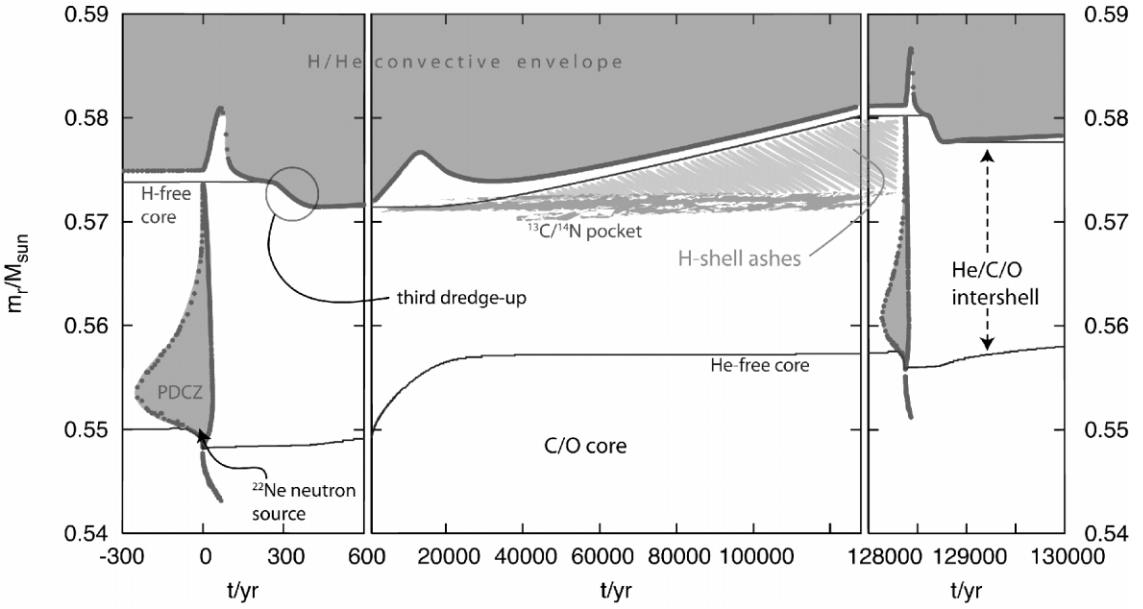

FIG. 6.—Time evolution of the Lagrangian position of convective regions (*solid gray*) and nuclear-burning shells (at the location of the H- and He-free cores, respectively). The time interval shown comprises one pulse cycle. Each dot along the boundaries of the convective regions corresponds to one time step in the model sequence. (Reprinted with permission, and with minor modifications, from Herwig 2005.)

engulfs more material from deeper layers. Eventually, a significant amount of material that has just been mixed and nuclear processed in the PDCZ is convectively mixed into the envelope and to the stellar surface by this third dredge-up.[1] At the end of the third dredge-up, the H-rich envelope and the ^{12}C-rich intershell layer are in direct contact, and any partial mixing, such as that due to overshooting (Herwig et al. 1997) or internal gravity waves (Denissenkov & Tout 2003), leads to a thin layer that contains both H and ^{12}C. As this layer resumes contraction after the thermal pulse and gradually heats up, H-shell burning eventually starts again. As part of that process, any partial-mixing layer of H and ^{12}C will produce an excess of ^{13}C. Detailed models have revealed that the neutron release in the ^{13}C pocket through the reaction $^{13}C(\alpha, n)^{16}O$ plays the most important role for the *s*-process in AGB stars (Gallino et al. 1998; Busso et al. 1999).

As the H shell burns outward during the interpulse phase, it leaves behind H-burning ashes, which mainly consist of ^{4}He. However, any CNO material in the envelope, including previously dredged-up ^{12}C, will be transformed into ^{14}N. In addition, the He-shell ashes contain fresh ^{56}Fe from the envelope. Just below the region with H-shell burning ashes is a thin layer that contains the ^{13}C pocket. The fact that the ^{13}C pocket contains a highly ^{14}N-rich region just above the ^{13}C abundance peak is extremely important in models that include shear mixing induced by differential rotation (Herwig et al. 2003a; Siess et al. 2004). The abundance distribution in the following PDCZ is therefore a mix of the H-shell ashes, the *s*-process–enriched material from the nuclear-processed ^{13}C pocket, and material that has been mixed and exposed to nucleosynthesis in the previous PDCZ. Obviously, the previous PDCZ is similarly a mix of these different components. Full stellar evolution calculations with sufficiently detailed nuclear networks can generate quantitative predictions for the intershell abundance distribution after many thermal pulses.

[1] The first and second dredge-up can occur earlier in the star's evolution, after the H- and He-core burning ceases.

3.1.2. Convective Extramixing and Rotation

Convective extramixing refers to a complex family of physical processes that lead to convection-induced mixing in stable layers adjacent to a convectively unstable zone. Although convective extramixing is sometimes simply referred to as overshooting, this term is reserved for the convective fluid motions that extend from unstable into stable layers and leave the thermodynamic stratification subadiabatic. If convective plumes that reach into the stable layers lead to an adiabatic stratification, the convective extramixing is referred to as penetration (Zahn 1991). However, yet another physical process can convectively induce mixing beyond the convective boundary. Convective motions may perturb the convective boundary, which can lead to the excitation of internal gravity waves (Press 1981). Such gravity modes can induce mixing in the radiative vicinity of convective boundaries (Garcia Lopez & Spruit 1991; Montalban 1994; Denissenkov & Tout 2003).

Over the past decade, hydrodynamic convection simulations

have generated additional insight into the relative importance of these convective extramixing processes. A very good example of overshooting has been observed in the shallow surface convection simulations by Freytag et al. (1996). Convective motions, both downdrafts and upflows, cross the convective boundaries without effort. The exponential decay of the convective motions stretches over a pressure scale height. Due to the very soft convective boundary, no gravity-wave excitation could be observed in these simulations. Hydrodynamic simulations by Bazan & Arnett (1998) and Young et al. (2005) have shown that the oxygen-shell convection in massive stars is a different regime. Although overshooting is also observed in these calculations, an equally important or maybe even dominating process for mixing is the excitation of gravity waves that generate turbulence in the radiative layers next to the convective boundary. The excitation of gravity waves is possible because the convective boundaries are much stiffer than in shallow surface convection. Qualitatively similar results have been found for He-shell flash convection in AGB stars by Herwig et al. (2006). Although convective extramixing has not been analyzed quantitatively, this study shows that overshooting motions are severely limited in their ability to cross the stiff convective boundary, especially the bottom boundary. However, the boundary stiffness leads to the excitation of high-amplitude gravity waves. The most recent simulations indicate that a small amount of mixing across the convective boundaries of the PDCZ exists, both at the top and bottom boundaries.

Convective extramixing at the bottom of the PDCZ has been included in AGB calculations as an exponential decay of the mixing-length theory convective diffusion coefficient (Herwig et al. 1997; Althaus et al. 2005b). Such extramixing leads to a higher temperature at the bottom of the PDCZ (Herwig 2000), with implications for the *s*-process–branching nucleosynthesis driven by the ^{22}Ne neutron source (Lugaro et al. 2003; Herwig et al. 2006). This limits the maximum amount of convective extramixing at the bottom of the PDCZ, but a detailed analysis to quantify this limit is not yet available. For the H-deficient post-AGB stars, another effect of this mixing is more important. The models predict that larger convective extramixing leads to a larger intershell abundance of ^{16}O. As we explain below, the observed oxygen abundance of H-deficient post-AGB stars is in very good agreement with AGB models that include this extramixing at the bottom of the PDCZ. The hydrodynamic properties of convective boundaries are intimately related to the predicted abundance patterns of H-deficient post-AGB stars.

The effect of stellar rotation, on the other hand, has not yet been studied in the same detail. Stellar models of AGB stars that include the effect of rotation have shown that the *s*-process nucleosynthesis efficiency in the ^{13}C pocket may be reduced compared to nonrotating models (Herwig et al. 2003a; Siess et al. 2004). Indirectly, convective extramixing at the bottom of the PDCZ could compensate for the reduced *s*-process efficiency in rotating AGB models through a larger ^{12}C intershell abundance (Herwig et al. 2006). While, as we discuss below, such a larger ^{12}C intershell abundance is in agreement with observations of H-deficient post-AGB stars, detailed models of this scenario are not yet available. It therefore seems that stellar rotation at this point is rather indirectly relevant for the interpretation of abundance patterns of H-deficient post-AGB stars.

3.2. Post-AGB Evolution

When the AGB star has lost all but approximately $10^{-2}\,M_{\odot}$ of its envelope mass, it starts the transition from the giant configuration to the white dwarf configuration (Schönberner 1979). The remaining envelope contracts and the star evolves at a constant luminosity to the hot stellar temperatures ($T_{\rm eff} >$ 30,000 K) that are required for central stars to ionize the planetary nebulae. Mass loss plays an important role in determining the transition velocity during this phase (Blöcker 2001). Eventually, H-shell burning stops and both the stellar luminosity and effective temperature start to decrease (Fig. 1). The star is about to enter the white dwarf cooling track. Up to this point, the star retains the ability to ignite a He-shell flash if the amount of He accreted from the H shell is large enough and the density in the He shell is high enough. Such a post-AGB He-shell flash will initiate a born-again evolution during which the star is reborn as a giant star. The basic concept of the born-again evolution scenario was established by Iben et al. (1983) and Schönberner (1983). It is noteworthy that Iben et al. (1983) have already speculated about the existence of two distinct born-again evolution channels, which we now refer to as the late thermal pulse (LTP) and the very late thermal pulse (VLTP). We add to those a variation of single-star evolution that may be able to produce H-deficient (possibly only mildly), hot post-AGB stars without a born-again evolution, the so-called AGB final thermal pulse (AFTP).

3.2.1. The Very Late Thermal Pulse

In the VLTP born-again evolution case, the PDCZ (Fig. 6) is able to penetrate into the remaining H-rich envelope, triggering a H-ingestion flash (HIF) that imposes its own nuclear burning and mixing signature on the subsequent evolution (Blöcker 2001; Herwig 2001b). This HIF is possible when the He-shell flash occurs very late in the post-AGB evolution, when the star is converging onto the white dwarf cooling track. At that time, the H-shell is inactive and provides no entropy jump that could prohibit convective instability below from spreading outward.

The time at which a He-shell flash can occur during the post-AGB evolution depends on the thermal pulse phase at which the star leaves the AGB. A departure too early in the cycle means that no He-shell flash will happen, and a departure too late in the cycle means a He-shell flash is triggered early in the post-AGB phase, when the H shell is still on, resulting in an LTP born-again evolution, rather than a VLTP.

Most born-again models that have been presented more recently are in fact VLTP models (Iben & MacDonald 1995).

The chain of events starts with the onset of the He-shell flash convection, which spreads over the entire intershell as the He-burning luminosity quickly increases in thermonuclear runaway. Close to the peak luminosity, the convective instability extends into the H-rich, unprocessed envelope. Protons are transported on the convective timescale into the hot, deep layers of the PDCZ. Eventually, the proton-rich material reaches temperatures that are high enough to allow the $^{12}C(p, \gamma)^{13}N$ reaction to proceed on the convective timescale. At this position within the PDCZ, the peak H-burning energy will be released. If we believe the one-dimensional stellar evolution models, the generation of energy leads to the formation of a separate convection zone driven by the H-burning energy and separated from the He-shell convection zone beneath it by a small radiative layer. The upper H-burning layer probably engulfs all of the material up to the stellar surface and burns its hydrogen content. Whatever traces of H that may be left will very likely be shed off by mass loss during the subsequent giant phase.

The VLTP model computations certainly are among the numerically more difficult stages of stellar evolution. Nevertheless, several improvements have been made in recent years. The VLTP model by Herwig et al. (1999) included a reliable, fully implicit numerical method for simultaneously solving the nuclear network and the time-dependent mixing equations. They also based their post-AGB evolution sequence on an AGB progenitor with convective extramixing (§ 3.1.2). In that way, the model could reproduce the observed high O abundance in [WC] and PG1159 stars. For the surface abundances, especially oxygen, Althaus et al. (2005b) come to the same conclusion.

When it became clear that Sakurai's object was in fact a VLTP case in which the born-again evolution from the pre-WD to the giant phase was witnessed in real time (§ 2.4), it also became clear that this star was not following the script that had been laid out by any of the previous calculations. The born-again evolution from the He-shell flash to the giant configuration has been observed to be only about 2 yr. However, all previous VLTP calculations predicted born-again evolution times that were a factor of 10 (Iben 1995) to 100 (Herwig et al. 1999) longer. An important difference between these two calculations is the numerical treatment of simultaneous burning and mixing, opacities, and metallicity, which collectively make a factor of 10 difference very plausible. For example, Lawlor & MacDonald (2003, their Table 2, col. [D–E]) show that the duration of the constant-luminosity part of the born-again evolution is about 3 times shorter for $Z = 0.001$ than for $Z = 0.02$. In any case, the important point is that these calculations do agree on the fact that Sakurai's object was retracing the evolution back to the AGB much faster than predicted by VLTP models. This indicated that the born-again evolution time is sensitive to the numerics, and also to the physics of burning and mixing and possibly other input physics.

Subsequently, a new generation of models of the VLTP has appeared. At the 2000 workshop "Sakurai's Object: What Have We Learned in the First Five Years?" held in Keele, UK, Lawlor & MacDonald (2002) presented VLTP tracks with two loops, similar to the track shown with dashed lines in Figure 1. However, the difference between these new models with double loops (see also Herwig 2003; Hajduk et al. 2005) and previous models was not initially clear. Herwig (2001a) then showed a connection between the convective mixing speed of surface H into the hot He- and ^{12}C-rich layers deeper inside and the born-again evolution time from the hot pre–white dwarf stage back to the giant configuration. The Lawlor & MacDonald (2002) and Herwig (2001a) models, as well as all later VLTP models, use some simultaneous treatment of nuclear burning and convective time-dependent mixing in which the sets of nuclear network equations in each mass shell are solved together with the diffusion equations for each species. Although the basic concept is similar in all of the more recent models, the details of the numerical solution technique differ, with possible consequences for the calculated born-again timescale.

Herwig (2001a) performed a series of tests for a 0.604 $M_\odot$ post-AGB star with a range of mixing speeds. Peak nuclear burning of ingested H with ^{12}C should occur where the nuclear and mixing timescales are the same. As the temperature strongly increases while protons convectively diffuse inward, the nuclear timescale decreases. For a reduced mixing velocity, the mixing timescale is larger and the position of equality of nuclear and mixing timescales is closer to the surface than with a faster mixing velocity, as predicted by the mixing-length theory. These models suggest that a solar-metallicity model with a mass of 0.604 $M_\odot$ could reproduce the born-again evolution time of Sakurai's object if the convective mixing speed were reduced by a factor 100.

Lawlor & MacDonald (2003) discuss the effect of reducing the mixing efficiency for three values: reduction by 10^2, 10^3, and 10^4. This may be a different regime than the one explored by Herwig (2001a), because they report a longer evolution timescale for a reduction factor of 10^4 than for 10^3. However, it should be noted that both of these models excluded some possibly important physics, such as the effect of μ-gradients on convective boundaries, or time-dependent convective energy transport.

The emerging picture, first fully described by Lawlor & MacDonald (2003), is that the VLTP evolution is a superposition of two flashes reflected in the double-loop morphology of the HRD track. The first fast born-again evolution is the result of the H-ingestion flash, whereas the second, longer lasting loop is driven by the He-shell flash that is still proceeding at the bottom of the intershell, largely unperturbed.

Even more recently, Althaus et al. (2005b) have presented new calculations of the VLTP that connect the VLTP event to the observational properties of PG1159 stars and DB and DQ white dwarfs. These calculations confirm the double-loop picture and feature a born-again evolution time of 50 yr. Miller Bertolami et al. (2006) investigate the dependence of the born-again times on additional physics, such as the convection theory and μ-gradients, and on numerical aspects, such as time resolution. The born-again time of their best model is 17 yr, without changing the mixing velocity ad hoc. They do confirm the

relation between mixing velocity and born-again time given by Herwig (2001a).

3.2.2. Discussion of the H-*Ingestion Mixing during the VLTP*

As the discussion in the previous subsection shows, the more recent stellar evolution studies of the VLTP show some agreement (e.g., the double-loop structure), as well as disagreement (e.g., the quantitative born-again timescale). All these calculations are based on some assumptions that are well founded in many phases of stellar evolution: spherical symmetry, the fact that convection can be described by time-averaged quantities as in mixing-length theory, and hydrostatic equilibrium. However, several or maybe all of these assumptions are invalid for the VLTP. The ingestion of hydrogen into the He-shell flash convection zone is a complicated multidimensional problem of turbulent convective-reactive fluid flow in which composition changes and reactive energy release are coupled to the dynamics (Dimotakis 2005).

There is considerable uncertainty in the treatment of nonreactive mixing at the H-rich–C-rich interface at the top of the convection zone. Convective rising plumes will perturb this interface, possibly penetrating a small distance. The perturbation of the boundary layer induces gravity waves (Herwig et al. 2006) that cause shear flows, possibly in the interaction with a small amount of convective penetration, and thereby turbulent mixing at this interface. This boundary mixing will be very important, because the much lower molecular weight of material in the H-rich stable layer will prevent unmixed blobs from being easily entrained into the He-shell flash convection zone. Nevertheless, as any stellar convection simulation shows, including those of the He-shell flash convection of Herwig et al. (2006), the overall convective flow morphology is dominated by structures that are roughly the size of the vertical extent of the convection zone. On these large vertical scales, confined downflows will eventually contain material with a significant H abundance. Nuclear energy from the $^{12}\mathrm{C}(p,\gamma)^{13}\mathrm{N}$ reaction is released in localized bursts at the vertical position where the temperature is large enough to reduce the nuclear burning timescale down to the local mixing timescale. This mixing timescale corresponds to the actual velocity in the downflow, not the rms-averaged value, which in fact corresponds well to the mixing-length velocity.

In most stellar evolution situations, the nuclear timescale is much longer than the convective timescale. This justifies the customary operator split between the convective mixing step and the nuclear-burning calculation. It also justifies the assumption that nuclear energy release is isotropic in the horizontal direction (or on spheres). However, in the H-ingestion flash, there are small and irregular parcels of energy production that coincide with the horizontal area of H-rich downflows. This breaks spherical symmetry.

The bursts of energy will locally add buoyancy and alter the convective flow patterns, deflecting focused downflows sideways or even reversing the flows. This corresponds to the notion derived from one-dimensional models that the energy release from the H-ingestion flash will lead to a split of the convective region associated with an impenetrable entropy barrier. Whether or not such a separation of convection zones will actually develop in real stars, and whether the one-dimensional mixing-length theory–based diffusion-burning models can account for this evolution phase at all, is uncertain, considering the many unknown aspects of the complicated reactive, turbulent mixing that dominates the above-sketched picture of the problem. This picture is based on our preliminary multidimensional hydrodynamic calculations of the H-ingestion problem.

In view of all these complications, it seems rather surprising that the more recent one-dimensional VLTP stellar evolution models agree to some extent with each other, and with the observed evolution of Sakurai's object at all. However, there is room for some doubt as to whether the current models describe the physics correctly on the level needed to understand the observations.

3.2.3. The Late Thermal Pulse and AGB Final Thermal Pulse

If the He-shell flash ignites during the earlier horizontal, constant-luminosity evolution, the star will follow a born-again evolution, but without a HIF. This variant of the post-AGB He-shell flash is the late thermal pulse (Blöcker 2001; Blöcker & Schönberner 1997). Although the LTP does not deplete H in the surface layer by nuclear burning, it will still develop a H-deficient surface composition (Herwig 2001b). This is achieved entirely by mixing. As the star inflates and the surface becomes cooler, envelope convection, which is characteristic for giant stars, emerges again. At this point a dredge-up event of the same form that follows the AGB thermal pulses will mix a very thin H-rich envelope layer of the order $10^{-4}\ M_{\odot}$ with a few $10^{-3}\ M_{\odot}$ of a H-free intershell layer. The result is H deficiency as a result of dilution. The LTP model of Herwig (2001b) predicts a H surface mass fraction of $X_{\mathrm{H}} = 0.02$.

The LTP has only a single loop back to the AGB, which proceeds on a long timescale, of the order 10^2 yr. In addition, there are differences in the abundance evolution that result from the fact that the LTP did not experience a HIF (§ 3.3). These include no Li production, no enhanced $^{14}\mathrm{N}$ abundance, and a larger $^{12}\mathrm{C}/^{13}\mathrm{C}$ ratio than in the VLTP HIF models. Unfortunately, there are no detailed LTP models available that include all of the relevant nucleosynthesis and a realistic treatment of the AGB progenitors.

The born-again scenario may imply that H-deficient CSPNs should have systematically older PNe, which is not the case (Górny 2001). In contrast, the appeal of the AFTP scenario is that it does not require that the central star evolve through a lengthy first CSPN phase and return to the AGB and the CSPN again. The AFTP leads to H deficiency at the last thermal pulse still on the AGB. By invoking some fine-tuning of the mass

loss, the envelope mass at the last AGB thermal pulse is so small that the star leaves the AGB immediately after the dredge-up following this last AGB thermal pulse. Because of this very small envelope mass, the dredge-up leads as in the LTP to a significant dilution of the H surface abundance.

The AFTP scenario is in contradiction to AGB stellar evolution studies of dredge-up toward the end of the AGB evolution, which assert that dredge-up stops when the envelope mass falls below a certain value. For example, a minimum envelope mass of 0.5 $M_\odot$ for dredge-up was reported by Straniero et al. (1997). However, dredge-up predictions in stellar evolution models are notoriously dependent on fine-tuning some mixing parameters, such as the mixing-length parameter or the overshooting parameter.

The two AFTP models of Herwig (2001b) were calculated with a mixing-length parameter of $\alpha_{\rm MLT} = 3.0$ and overshooting. At the time of the last AGB thermal pulse, the envelope mass was 3×10^{-2} $M_\odot$ and 4×10^{-3} $M_\odot$, and the dredged-up mass was in both cases 6×10^{-3} $M_\odot$. This resulted in H abundances at the surface of the post-AGB star of $X_{\rm H} = 0.55$ and 0.17, respectively. This is much larger than the H abundance observed in PG1159 stars. However, the AFTP model may explain quite naturally the "hybrid" PG1159 stars, which are H deficient yet have much larger H abundances than the typical PG1159 and [WC]-CSPN stars (Tables 1 and 2; Napiwotzki et al. 1991).

The main problem with the AFTP scenario seems to be a missing mechanism that favors a zero (or very small) pulse phase for the departure from the AGB. Somehow, the thermal pulse must trigger enhanced mass loss that in turn enhances the probability of a departure at phase close to zero. The typical AGB mass-loss formulae do not provide such a mechanism and would lead to a very low probability of such an event.

De Marco et al. (2003b) considered the possibility that swallowing a planet or a very low mass companion star could eject the envelope with high probability during the temporary, significant radius increase induced by the thermal pulse. The multidimensional simulations showed that envelope ejection is indeed possible. This would initialize the departure from the AGB. Clearly, this interesting possibility needs more investigation, and such efforts are under way.

3.2.4. The HRD Tracks of Post-AGB Evolution and the Importance of the AGB Progenitor Evolution

The evolution tracks of an undisturbed H-normal post-AGB evolution (no TP), an AFTP track, and a VLTP track are compared in Figure 7. All three tracks have been started from the same tip-AGB model that was evolved through all previous evolution phases from a 2 $M_\odot$ main-sequence model. The stellar mass at the time of departure from the AGB is 0.604 $M_\odot$. The comparison shows that surface abundance has no effect before the "knee" (the hottest point in the track) and only a small effect after the knee, where the H-normal track is slightly

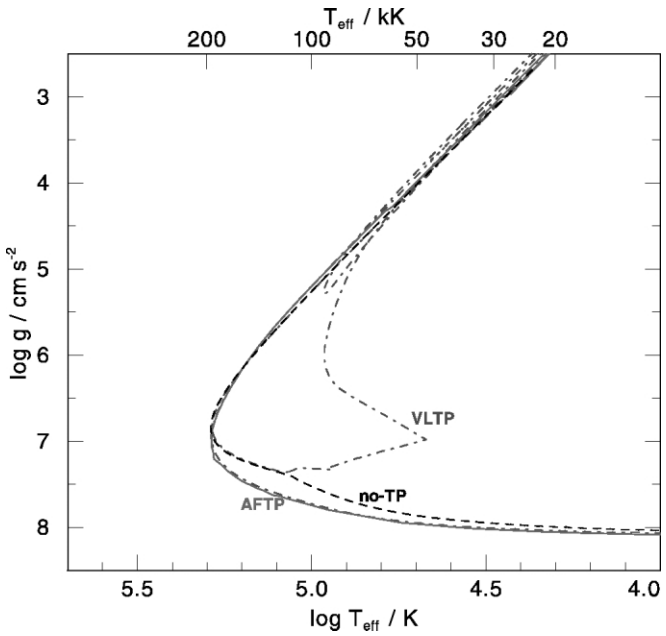

FIG. 7.—Comparison of three different evolution channels in the log g– log $T_{\rm eff}$plane for a 0.604 $M_\odot$ post-AGB star that had a main-sequence mass of 2 $M_\odot$ and evolved through about a dozen thermal pulses with dredge-up. [*See the electronic edition of the PASP for a color version of this figure*.]

cooler for a given log g. However, this difference should not be overemphasized, because it is largely due to a "kink" in the track that reflects the onset of the reignition of the He shell. In the no-TP track, the He-shell flash runaway does not develop. For the HRD track after the knee, it does not seem to matter how the star became H deficient. The AFTP and the final CSPN evolution of the VLTP have identical tracks. This indicates that H-normal CSPN tracks can be used as a tool to determine masses from spectroscopic stellar parameters in the absence of an homogeneous grid of H-deficient tracks.

Another point that is evident from the comparison of tracks in Figure 2 seems to be more important for accurate mass determinations. This figure shows older tracks from Schönberner (1983), Blöcker (1995), and Wood & Faulkner (1986), as well as our newer VLTP track, which is also shown in Figure 7. While the 0.605 $M_\odot$ track from Blöcker (1995) and the 0.6 $M_\odot$ track from Wood & Faulkner (1986) show good agreement, the new 0.604 $M_\odot$ track is $\Delta \log T_{\rm eff} = 0.1$–$0.15$ hotter at and below the knee. This is even more surprising, since the same code (although with some differences concerning nucleosynthesis and mixing) has been used for the 0.605 and 0.604 $M_\odot$ models.

The reason for this HRD track difference is a different dredge-up or mass-loss history, or both, in the AGB progenitor evolution. For the new 0.604 $M_\odot$ track, the AGB progenitor evolution includes a complete sequence of thermal pulses, a large number of which are followed by third dredge-up mixing events. These dredge-up events lead to a smaller effective core growth, while the properties of the core itself, in particular the

radius, depend to a large extent on the increasing degeneracy of the C-O core (Herwig et al. 1998; Mowlavi 1999). If an AGB evolution sequence experiences many efficient third dredge-up events, the resulting post-AGB star appears in the HRD as a slightly more massive star compared to the same core mass post-AGB stellar model that has an AGB thermal pulse history of inefficient or no dredge-up.

Mass loss can have a similar effect, because it determines the age of the core for a given initial mass at the tip of the AGB (Blöcker & Schönberner 1990). This was shown in detail by Blöcker (1995, his Fig. 10), who calculated two post-AGB tracks with identical mass (0.84 $M_\odot$): one with a 5 $M_\odot$ main-sequence progenitor, and one initially with 3 $M_\odot$. In order for the 3 $M_\odot$ model to reach such a high core mass, a smaller mass-loss rate than for the 5 $M_\odot$ track was adopted. In this way, the core had a long time to grow through shell burning before the envelope loss forced the AGB departure. The result is a more degenerate, more compact, and consequently hotter post-AGB stellar model with the 3 $M_\odot$ progenitor compared to the post-AGB model with the 5 $M_\odot$ progenitor.

In summary, if CSPN tracks are computed for the purpose of determining masses (or fading times), the third dredge-up and the mass loss during the progenitor evolution must be accurately taken into account.

3.3. Surface Abundance Predictions for H-deficient Post-AGB Stars

If we interpret H-deficient post-AGB stars, such as PG1159 stars or [WC]-CSPNs, as the bare cores of former AGB stars exposed by the born-again evolution or an AFTP evolution, then the surface abundance of these stars is a superposition of the intershell abundance of the progenitor AGB star at the last thermal pulse on the AGB and any modification in particular that the violent burning and mixing associated with the H-ingestion flash of the VLTP may have caused. We discuss below the surface abundance predictions for the elements that have been observed so far, taking into account both of these contributions.

3.3.1. Carbon and Oxygen

During the He-shell flash, the 3α reaction that transforms three ^{4}He into one ^{12}C is the dominant source of energy. The layers immediately below the PDCZ contain an amount of ^{16}O from the ^{12}C(α, γ)^{16}O reaction that increases with depth. Starting with the earliest models of thermal pulse AGB stars (Schönberner 1979), it has been consistently found that without convective extramixing, the ^{16}O abundance is 0.01–0.02 and the ^{12}C abundance is 0.2–0.25 in the intershell, with the remainder being $\sim$0.75 ^{4}He.

More recently, models with convective extramixing in the form of a parameterized exponential overshoot at the bottom of the PDCZ have been constructed (Herwig et al. 1997; Herwig 2000; Althaus et al. 2005b). These models agree quantitatively that such extramixing leads to a systematically larger ^{16}O and ^{12}C abundance in the PDCZ. Herwig (2000) showed that the efficiency of convective extramixing is proportional to the intershell ^{16}O abundance. In addition, there is an evolution of the ^{16}O abundance with pulse number, initially rising and then reaching a maximum value after a few thermal pulses, and decreasing toward a plateau at the last thermal pulses. For the evolution sequence initially with 3 $M_\odot$, Herwig (2000) finds at the last computed thermal pulse an intershell abundance of $X(^{16}\mathrm{O}) = 0.18$ and $X(^{12}\mathrm{C}) = 0.41$. For a sequence with 2.7 $M_\odot$ initially, Althaus et al. (2005b) find $X(^{16}\mathrm{O}) = 0.23$ and $X(^{12}\mathrm{C}) = 0.50$. Presumably, this difference is due to the smaller number of thermal pulses in Althaus et al. (2005b) compared to Herwig (2000). As mentioned above, the ^{16}O intershell abundance goes through a maximum (corresponding to a minimum for ^{4}He) before approaching a plateau. The Althaus et al. (2005b) intershell abundance may correspond to a thermal pulse closer to that maximum.

3.3.2. Nitrogen

Nitrogen is produced in AGB stars by H-shell burning on envelope material enriched by carbon dredge-up after previous thermal pulses. In low-mass AGB stars, the H-burning shell burns most CNO matter in the envelope material it consumes into ^{14}N. Therefore, the ashes from H-shell burning (see Fig. 6) contain more ^{14}N with each dredge-up pulse, which is mixed in the next He-shell flash convection zone. In the He-burning shell during the flash, this ^{14}N is destroyed and forms ^{18}O and ^{22}Ne (see below). The models predict that the intershell of AGB stars at the end of their evolution is practically free of ^{14}N.

In massive AGB stars, ^{14}N is produced in the envelopes by hot bottom burning (Sackmann & Boothroyd 1992). The dredged-up carbon in the envelope is transformed by two *p*-captures into ^{14}N, because part of the H-burning shell is included in the convective envelope. Therefore, we expect in the more massive post-AGB stars of roughly solar metallicity a nitrogen mass fraction of 1% to maybe a few percent in the H-rich envelope at the time of departure from the AGB.

The nitrogen evolution is different for the LTP and VLTP. The LTP will only dilute some intershell material with the remaining small amount of envelope material. Even if the progenitor has evolved through the hot bottom burning phase, the nitrogen abundance will be at most roughly 0.1%. If the star evolves through a VLTP, nitrogen is produced by the H ingestion and may be as high as a few percent. The absence or presence of N should be a reliable indicator of a LTP or VLTP event.

3.3.3. Neon

During each interpulse phase, the H shell builds a layer of ashes that is engulfed in the following PDCZ. These H-shell ashes contain mainly ^{4}He, with an important modification of

the CNO abundances. All CNO, whether from the stellar initial abundance or dredged up after a previous thermal pulse, will be mostly transformed into ^{14}N. This ^{14}N is exposed to the high He-burning temperature ($T \approx 3 \times 10^8$ K) at which two α-captures lead to the formation of ^{18}O first, and then ^{22}Ne. Depending on mass, some ^{22}Ne is destroyed by the neutron-producing reaction ^{22}Ne(α, n)^{25}Mg. For low-mass AGB stars with initial masses of around 1.5 $M_\odot$, the ^{22}Ne depletion is small (≈3%) only because the peak temperature at the base of the PDCZ is not reaching high enough values, $>3 \times 10^9$ K. Stellar evolution models agree that the mass fraction of ^{22}Ne is about 2%. A certain spread in the observed values is expected. The production of ^{22}Ne is larger in cases with more dredge-up of ^{12}C. The destruction of ^{22}Ne through α-capture increases with initial mass. As a trend, the intershell ^{22}Ne should decrease with increasing initial stellar mass.

3.3.4. Iron and Nickel

Fresh ^{56}Fe is added to the intershell with the H-shell ashes, which are processed envelope material and therefore contain the Fe abundance of the envelope. In the PDCZ, ^{56}Fe will be reduced by neutron capture and transformed into Ni if the ^{22}Ne neutron source is active; i.e., ^{56}Fe reduction will be more efficient in higher core-mass AGB stars. However, as is the case for many other species, the evolution of intershell ^{56}Fe with increasing pulse number depends sensitively on the dredge-up history, which in turn seems in model calculations to be related to assumptions about convective extramixing (Mowlavi 1999).

Preliminary models by Herwig et al. (2003b) show that the ^{56}Fe depletion in the PDCZ at the last thermal pulse of a 3 $M_\odot$ star varies significantly depending on stellar evolution model assumptions. For a thermal pulse AGB sequence with convective extramixing, showing very efficient third dredge-up and high peak temperatures at the base of the PDCZ, the ^{56}Fe depletion is approximately 0.7 dex, whereas a model without convective extramixing predicts an ^{56}Fe depletion of only 0.2 dex. In both cases, all heavier isotopes of Fe and Ni are significantly overabundant. An additional depletion of Fe and production of Ni may occur during the late thermal pulse (§ 3.2.1). In any case, the unmistakable signature of Fe depletion due to *n*-capture nucleosynthesis is the simultaneous increase of Ni and corresponding decrease of the Fe/Ni ratio. While the solar ratio is about 20, material that has experienced a significant neutron exposure would show a ratio closer to the *s*-process quasi–steady state of ≈3.

3.3.5. Fluorine

Jorissen et al. (1992) have observed high enhancements of fluorine in AGB stars. They found a correlation between F enhancement and the C-O ratio, which is a strong indication that F is produced in the intershell and is mixed to the surface during the third dredge-up. Observations show that thermal pulses cause a tenfold increase in ^{19}F.

The nucleosynthesis path to ^{19}F first involves production of ^{15}N, which requires a neutron source: ^{14}N(n, p)^{14}C(α, γ)^{18}O(p, α)^{15}N. This chain of reaction occurs during the interpulse phase. The neutrons are provided by ^{13}C in both the H-shell ashes and in the ^{13}C pocket. For a certain range of mixing efficiencies, rotation-induced mixing may enhance the production of ^{15}N (Herwig et al. 2003a). ^{15}N produced in either way is then engulfed by the PDCZ. Fluorine is produced by ^{15}N(α, γ)^{19}F. The limiting factor in this scenario is the efficient ^{19}F(α, p)^{22}Ne reaction. ^{19}F production exceeds destruction only in a narrow temperature range at the base of the PDCZ, between 2.2×10^8 and 2.6×10^8 K (Mowlavi et al. 1996).

Lugaro et al. (2004) show that the ^{19}F abundance in the He intershell after the last thermal pulse has a maximum between 2 and 3.5 $M_\odot$, depending on metallicity. For $Z = 0.02$ and 0.008, the intershell abundance reaches a maximum between 150 and 290 times solar [$X(^{19}\mathrm{F})_\odot = 4.1 \times 10^{-7}$] at 3.5 and 3.0 $M_\odot$, respectively. However, for cores with larger or smaller initial mass, the ^{19}F intershell abundance may be as small as the solar value.

Within an evolution sequence of thermal pulses for a given initial mass, and even within an individual thermal pulse, the ^{19}F intershell shows a considerable spread. The variation from pulse to pulse means that a quantitative comparison with observed ^{19}F values in H-deficient post-AGB stars depends on details of the entire AGB evolution, including for example an accurate description of mass loss and dredge-up to correctly model the total number of thermal pulses. The spread within one He-shell flash convection event means that there may be observable differences in the ^{19}F abundance between the VLTP with H ingestion and the LTP born-again evolutions.

Finally, it should be mentioned that Lugaro et al. (2004) find that nuclear reaction rate uncertainties, in particular for the ^{14}C(α, γ)^{18}O and ^{19}F(α, p)^{22}Ne reactions, significantly limit the accuracy of stellar model predictions of ^{19}F.

3.3.6. Silicon, Phosphorus, and Sulfur

These three elements have a too high Coulomb barrier to be altered by charged-particle reactions in AGB stars. This leaves only neutron captures to be considered for elemental abundance shifts of Si, S, and P. It is well known from the study of presolar grains that the neutron fluxes in AGB stars modify the ratios of the three stable Si isotopes (Lugaro et al. 1999). However, the elemental abundance of Si is dominated by the lightest isotope, ^{28}Si, which in the solar abundance distribution accounts for approximately 90% of the elemental Si abundance. Neutron exposure in AGB stars will shift a small fraction of ^{28}Si to ^{29}Si and ^{30}Si, but the elemental abundance changes only very little in the He intershell of AGB stars. Therefore, a solar Si abundance is expected in hot, H-deficient post-AGB stars.

For phosphorus, the model calculation initially with 3 $M_\odot$

predicts an enhancement in the intershell at the end of the AGB that is sensitive to the assumptions about convective extramixing. The expected range is from 4 times solar without extramixing to ~25 times solar with extramixing. As discussed in § 3.1.2, the respective mixing algorithm contains a free efficiency parameter. We consider the efficiency chosen in this model to be an upper boundary. As is the case for ^{19}F, the He-shell flash nucleosynthesis can be sensitive to the initial mass. A systematic evaluation of the P intershell abundance as a function of mass and metallicity is not yet available.

The same models predict a small deficiency in S in the intershell at the end of the AGB, ranging from 0.6 times solar with convective extramixing to 0.9 times solar for the standard model. A more systematic evaluation of the intershell abundance evolution of S and P should include the neutron capture cross section uncertainties. However, in general the uncertainties for these stable isotopes are typically less than 10% (Bao et al. 2000).

3.3.7. Lithium

Although Li cannot be observed in hot post-AGB stars, the observed Li overabundance in Sakurai's object is an important hint. The production of this fragile element in the form of its heavy isotope ^{7}Li is usually associated with hot bottom burning in massive AGB stars (Scalo et al. 1975; Sackmann & Boothroyd 1992). Enhanced extramixing in red giant branch stars induced by tidal synchronization or swallowing of a giant planet has been proposed as another source of ^{7}Li (Denissenkov & Herwig 2004). Both of these production sites are based on the ^{7}Be transport processes. ^{3}He and ^{4}He form ^{7}Be, which becomes ^{7}Li through a largely temperature-insensitive e^- capture on a timescale of approximately 1 yr. If the production region of ^{7}Be is convectively connected to cooler layers, as in envelope convection that reaches into the H-burning shell in hot bottom burning, then ^{7}Be is transported out of the hot layers, and the resulting ^{7}Li can survive because it is not immediately destroyed by *p*-captures.

Herwig & Langer (2001) have shown that if ^{3}He in the envelope has not been destroyed by one of the two processes mentioned above (which is likely for most low-mass AGB stars with initial masses below ~3.5 $M_\odot$), then copious amounts of ^{7}Li can be produced in the hydrogen ingestion flash. They refer to this process as hot, H-deficient ^{3}He burning. The reason is somewhat different from the ^{7}Be transport mechanism, in which ^{7}Be is transported out of the hot, *p*-rich, and therefore ^{7}Li-hostile environment quickly enough. In the HIF, the amount of ingested H is strictly limited, and in addition to H, ^{3}He is ingested into the He-shell flash convection zone. This ^{3}He quickly reacts with ^{4}He and forms ^{7}Be, which then has to wait for an e^- capture to become ^{7}Li. This waiting period is long enough for all the protons to be rapidly consumed by ^{12}C. By the time ^{7}Li appears, no protons are available for Li destruction, leading to a net production of ^{7}Li. Current models only account qualitatively for the processes involved. In a one-zone model, Herwig & Langer (2001) find a maximum mass fraction of $X(^7\mathrm{Li}) = 3 \times 10^{-6}$, which corresponds to ~2.5 dex more than the solar system meteoritic value. We expect that the surface overabundance of Li in a realistic multizone model would be much smaller.

^{7}Li production in a HIF has been recently confirmed by Iwamoto et al. (2004) in the context of He-shell flashes in extremely metal-poor AGB stars. In this context, it is interesting to note that Cameron & Fowler (1971) in fact originally proposed the ^{7}Be transport mechanism motivated by the first HIF models by Schwarzschild & Härm (1967), which were not, however, reproduced by subsequent models that included radiation pressure.

4. COMPARISON OF OBSERVATION AND THEORY

In §§ 2 and 3, we have presented in detail the elemental abundances observed in PG1159 and [WC] stars, as well as the surface abundances predicted from stellar evolution models. How do they compare?

Hydrogen.—The observed H deficiency is in accordance with evolution models of the born-again scenario. In the VLTP models, H is ingested and burned and disappears completely. An LTP event causes mixing of the H-rich envelope with the intershell so that H is diluted down to a mass fraction of the order 0.02. This is close to the observational limit. The relatively high H abundances in the hybrid PG1159 stars and some [WC] stars (of the order 0.15) are explained by AFTP models.

Helium, carbon, and oxygen.—These are the main constituents of the intershell region of AGB stars, and the model abundances generally agree with the observed abundances in PG1159 and [WC] stars. The spread of observed relative He/C/O ratios can in part be explained by differences in stellar mass and the different number of thermal pulses experienced by objects that even have equal total mass (the latter being a consequence of potentially different AGB mass loss, for example, as a result of rotation). However, we think that a few extreme cases of He/C/O ratios remain unexplained; in particular, objects with relatively low O abundance (of order 0.01) and simultaneously high C abundance (of order 0.5). One speculative scenario has been sketched by De Marco et al. (2003a). If the AGB star has a low-mass stellar or planetary companion at a distance of 1–2 AU, it would be engulfed during the radius peak induced by the first thermal pulse. The transfer of orbital energy into the AGB envelope may eject the envelope and lead to a departure from the AGB. According to Herwig (2000), the intershell O abundance is very low after the first thermal pulse, even if overshooting has been applied. If such an evolution later involves a VLTP or LTP, a PG1159 star with a very low O abundance would result. A similar evolution could result from a low-mass star that naturally leaves the AGB just before the first thermal pulse (Miller Bertolami & Althaus 2006).

Isotopic ratios cannot be measured in hot post-AGB stars.

However, both the $^{12}C/^{13}C$ and the C/N ratios of our VLTP model are in good agreement with the observations of Sakurai's object.

Nitrogen.—The observations show a wide range of N abundance, from very low upper limits ($<3 \times 10^{-5}$ in HS 1517+7403) to mass fractions of 1%–2%, in agreement with predictions for LTP and VLTP evolution, respectively. Intermediate abundance levels could in some cases be associated with higher stellar mass.

Neon.—The observed high Ne abundances (of the order 0.02) agree well with the model predictions.

Fluorine.—The rich diversity of F abundances observed in PG1159 stars (from solar up to 250 times solar) is explained by models with different stellar masses leading to different F production efficiencies.

Silicon.—The Si abundance in the evolution models is almost unchanged, so that a solar abundance is expected. Only few abundance analyses are available. PG1159 stars display the expected Si abundance, while surprisingly strong overabundances (up to 40 times solar) have been found in some [WCL] stars.

Phosphorus.—Theoretical predictions and observational data are scarce. Current models are consistent with P overabundances of up to 4–25 times solar. Preliminary results from two PG1159 stars indicate roughly solar abundances.

Sulfur.—Preliminary abundance determinations in PG1159 stars suggest a wide spread, ranging between 0.01 and 1 times solar. These results need to be confirmed by further analyses. As in the case of phosphorus, systematic investigations with evolution models are lacking, but current models predict only slight (0.6 solar) S depletion.

Lithium.—The Li abundance cannot be determined in hot objects, so no conclusions can be drawn from PG1159 and [WC] stars. However, Sakurai's object shows a large Li abundance. As discussed in previous sections, this Li cannot have survived from an earlier phase, and is a strong additional hint that Sakurai's object did in fact evolve through a VLTP.

Iron and nickel.—The observed Fe deficiency in PG1159 and [WC] stars is explained by neutron captures on ^{56}Fe. The consequent increase of Ni abundance cannot be confirmed or contradicted with current observational material. However, Sakurai's object indeed exhibits a strongly subsolar Fe/Ni ratio that is quantitatively in agreement with model estimates.

To conclude, elemental abundances predicted by born-again evolutionary models (for the LTP and VLTP) and by AGB final thermal pulse (AFTP) models can explain most observational results from PG1159 and [WC] star analyses. The model surface abundances largely reflect the intershell abundance of the AGB progenitor. From the good qualitative and quantitative agreement between observed and predicted abundances, we conclude that [WC] and PG1159 stars generally display on their surface the intershell material of the AGB progenitor. For this reason, detailed quantitative spectroscopic investigations of these hot post-AGB stars can be used as a tool to study the nuclear production site of the He intershell in AGB stars. Such a tool is particularly useful because the AGB interior is otherwise obviously inaccessible to direct observation. It is hoped that new observations and analyses of these H-deficient post-AGB stars will contribute to an even more complete picture of the nuclear astrophysical processes in AGB stars.

F. H. would like to thank Lars Koesterke for his early support in numerical methods for burning and mixing in one-dimensional born-again stellar evolution models. He would also like to thank Bernd Freytag for his delightful collaboration on stellar interior convection hydrodynamic simulations, and Orsola De Marco for many enlightening discussions about CSPNs and other things. K. W. thanks Stefan Dreizler, Uli Heber, and Thomas Rauch for their enduring close collaboration. We would like to thank Maria Lugaro for her help with preliminary estimates on P and S abundance predictions. Comments on an earlier version of this paper by Orsola De Marco, Wolf-Rainer Hamann, Thomas Rauch, and Detlef Schönberner are gratefully acknowledged. This work was funded in part under the auspices of the US Department of Energy under the ASC program and the LDRD program (20060357ER) at Los Alamos National Laboratory. It was also funded in part by the German Science Foundation (DFG) and the German Aerospace Center (DLR).

REFERENCES

Acker, A., & Neiner, C. 2003, A&A, 403, 659
Althaus, L. G., Miller Bertolami, M. M., Córsico, A. H., García-Berro, E., & Gil-Pons, P. 2005a, A&A, 440, L1
Althaus, L. G., Serenelli, A. M., Panei, J. A., Córsico, A. H., García-Berro, E., & Scóccola, C. G. 2005b, A&A, 435, 631
Asplund, M., Gustafsson, B., Lambert, D. L., & Rao, N. K. 2000, A&A, 353, 287
Asplund, M., Lambert, D. L., Kipper, T., Pollacco, D., & Shetrone, M. D. 1999, A&A, 343, 507
Bao, Z. Y., Beer, H., Käppeler, F., Voss, F., Wisshak, K., & Rauscher, T. 2000, At. Data Nucl. Data Tables, 76, 70
Barlow, M. J., & Hummer, D. G. 1982, in IAU Symp. 99, Wolf-Rayet Stars: Observations, Physics, Evolution, ed. C. de Loore & A. Willis (Dordrecht: Reidel), 387
Bauer, F., & Husfeld, D. 1995, A&A, 300, 481
Bazan, G., & Arnett, D. 1998, ApJ, 496, 316
Blöcker, T. 1995, A&A, 299, 755
———. 2001, Ap&SS, 275, 1
Blöcker, T., & Schönberner, D. 1990, A&A, 240, L11
———. 1997, A&A, 324, 991
Bond, H. E., et al. 1996, AJ, 112, 2699
Busso, M., Gallino, R., & Wasserburg, G. J. 1999, ARA&A, 37, 239
Cameron, A. G. W., & Fowler, W. A. 1971, ApJ, 164, 111
Clayton, G. C., & De Marco, O. 1997, AJ, 114, 2679
Córsico, A. H., & Althaus, L. G. 2005, A&A, 439, L31
Cox, A. N. 2003, ApJ, 585, 975
Crowther, P. A., de Marco, O., & Barlow, M. J. 1998, MNRAS, 296, 367

De Marco, O., & Barlow, M. J. 2001, Ap&SS, 275, 53
De Marco, O., Sandquist, E. L., Mac Low, M.-M., Herwig, F., & Taam, R. E. 2003a, in Rev. Mexicana Astron. Astrofis. Ser. Conf. 18, The Eighth Texas-Mexico Conference on Astrophyiscs: Energetics of Cosmic Plasmas, ed. M. Reyes-Ruiz & E. Vazquez-Semadeni (Mexico City: UNAM), 24
———. 2003b, in Rev. Mexicana Astron. Astrofis. Conf. Ser. 15, Winds, Bubbles, and Explosions, ed. S. J. Arthur & W. J. Henney (Mexico City: UNAM), 34
Denissenkov, P. A., & Herwig, F. 2004, ApJ, 612, 1081
Denissenkov, P. A., & Tout, C. A. 2003, MNRAS, 340, 722
Dimotakis, P. E. 2005, Annu. Rev. Fluid Mech., 37, 329
Dreizler, S. 1998, Baltic Astron., 7, 71
Dreizler, S., & Heber, U. 1998, A&A, 334, 618
Dreizler, S., Werner, K., & Heber, U. 1995, in White Dwarfs, ed. D. Koester & K. Werner (LNP 443; Heidelberg: Springer), 160
Duerbeck, H. W., & Benetti, S. 1996, ApJ, 468, L111
Duerbeck, H. W., Benetti, S., Gautchy, A., van Genderen, A. M., Kemper, C., Lillier, W., & Thomas, T. 1997, AJ, 114, 1657
Duerbeck, H. W., et al. 2000, AJ, 119, 2360
Fedrow, J., Clayton, G., Crowther, P., & Kerber, F. 2005, AAS Meeting 207, 182.20
Fogel, J., Marco, O. D., & Jacoby, G. 2003, in IAU Symp. 209, Planetary Nebulae: Their Evolution and Role in the Universe, ed. S. Kwok, M. Dopita, & R. Sutherland (San Francisco: ASP), 235
Freytag, B., Ludwig, H.-G., & Steffen, M. 1996, A&A, 313, 497
Fu, J.-N., & Vauclair, G. 2006, A&A, submitted
Fujimoto, M. Y. 1977, PASJ, 29, 331
Gallino, R., Arlandini, C., Busso, M., Lugaro, M., Travaglio, C., Straniero, O., Chieffi, A., & Limongi, M. 1998, ApJ, 497, 388
Garcia Lopez, R. J., & Spruit, H. C. 1991, ApJ, 377, 268
Gautschy, A. 1997, A&A, 320, 811
Gautschy, A., Althaus, L. G., & Saio, H. 2005, A&A, 438, 1013
Gehrz, R. D., Woodward, C. E., Temim, T., Lyke, J. E., & Mason, C. G. 2005, ApJ, 623, 1105
Gonzalez, G., Lambert, D. L., Wallerstein, G., Rao, N. K., Smith, V. V., & McCarthy, J. K. 1998, ApJS, 114, 133
Górny, S. K. 2001, Ap&SS, 275, 67
Gräfener, G., Hamann, W.-R., & Peña, M. 2003, in IAU Symp. 209, Planetary Nebulae: Their Evolution and Role in the Universe, ed. S. Kwok, M. Dopita, & R. Sutherland (San Francisco: ASP), 577
Grevesse, N., & Sauval, A. J. 2001, in Encyclopedia of Astronomy and Astrophysics, ed. P. Murdin (Bristol: IoP), 2453
Hajduk, M., et al. 2005, Science, 308, 231
Hamann, W.-R. 1997, BAAS, 31, 1400
———. 2003, in IAU Symp. 209, Planetary Nebulae: Their Evolution and Role in the Universe, ed. S. Kwok, M. Dopita, & R. Sutherland (San Francisco: ASP), 203
Hamann, W.-R., Peña, M., Gräfener, G., & Ruiz, M. T. 2003, A&A, 409, 969
Hamann, W.-R., Todt, H., & Gräfener, G. 2005, in AIP Conf. Proc. 804, Planetary Nebulae as Astronomical Tools, ed. R. Szczerba, G. Stasińska, & S. K. Górny (New York: AIP), 153
Heap, S. R. 1975, ApJ, 196, 195
Herald, J. E., Bianchi, L., & Hillier, D. J. 2005, ApJ, 627, 424
Herwig, F. 2000, A&A, 360, 952
———. 2001a, ApJ, 554, L71
———. 2001b, Ap&SS, 275, 15
———. 2003, in IAU Symp. 209, Planetary Nebulae: Their Evolution and Role in the Universe, ed. S. Kwok, M. Dopita, & R. Sutherland (San Francisco: ASP), 111
———. 2005, ARA&A, 43, 435
Herwig, F., Blöcker, T., Langer, N., & Driebe, T. 1999, A&A, 349, L5
Herwig, F., Blöcker, T., Schönberner, D., & El Eid, M. F. 1997, A&A, 324, L81
Herwig, F., Freytag, B., Hueckstaedt, R. M., & Timmes, F. X. 2006, ApJ, in press
Herwig, F., & Langer, N. 2001, Nucl. Phys. A, 688, 221
Herwig, F., Langer, N., & Lugaro, M. 2003a, ApJ, 593, 1056
Herwig, F., Lugaro, M., & Werner, K. 2003b, in IAU Symp. 209, Planetary Nebulae: Their Evolution and Role in the Universe, ed. S. Kwok, M. Dopita, & R. Sutherland (San Francisco: ASP), 85
Herwig, F., Schönberner, D., & Blöcker, T. 1998, A&A, 340, L43
Hügelmeyer, S. D., et al. 2006, A&A, submitted
Iben, I., Jr. 1995, Phys. Rep., 250, 1
Iben, I., Jr., Kaler, J. B., Truran, J. W., & Renzini, A. 1983, ApJ, 264, 605
Iben, I., Jr., & MacDonald, J. 1995, in White Dwarfs, ed. D. Koester & K. Werner (LNP 443: Heidelberg: Springer), 48
Iben, I., Jr., & Renzini, A. 1983, ARA&A, 21, 271
Iwamoto, N., Kajino, T., Mathews, G. J., Fujimoto, M. Y., & Aoki, W. 2004, ApJ, 602, 378
Jahn, D. 2005, thesis, Univ. Tübingen
Jorissen, A., Smith, V. V., & Lambert, D. L. 1992, A&A, 261, 164
Kawaler, S. D., & Bradley, P. A. 1994, ApJ, 427, 415
Kawaler, S. D., et al. 1995, ApJ, 450, 350
———. 2004, A&A, 428, 969
Koesterke, L. 2001, Ap&SS, 275, 41
Koesterke, L., Dreizler, S., & Rauch, T. 1998, A&A, 330, 1041
Koesterke, L., & Hamann, W.-R. 1997a, in IAU Symp. 180, Planetary Nebulae, ed. H. J. Habing & H. J. G. L. M. Lamers (Dordrecht: Kluwer), 114
———. 1997b, A&A, 320, 91
Koesterke, L., & Werner, K. 1998, ApJ, 500, L55
Lawlor, T. M., & MacDonald, J. 2002, Ap&SS, 279, 123
———. 2003, ApJ, 583, 913
Lechner, M. F. M., & Kimeswenger, S. 2004, A&A, 426, 145
Leuenhagen, U., & Hamann, W.-R. 1998, A&A, 330, 265
Lugaro, M., Herwig, F., Lattanzio, J. C., Gallino, R., & Straniero, O. 2003, ApJ, 586, 1305
Lugaro, M., Ugalde, C., Karakas, A. I., Görres, J., Wiescher, M., Lattanzio, J. C., & Cannon, R. C. 2004, ApJ, 615, 934
Lugaro, M., Zinner, E., Gallino, R., & Amari, S. 1999, ApJ, 527, 369
Méndez, R. H. 1991, in IAU Symp. 145, Evolution of Stars: The Photospheric Abundance Connection, ed. G. Michaud & A. Tutukov (Dordrecht: Kluwer), 375
Metcalfe, T. S., Nather, R. E., Watson, T. K., Kim, S.-L., Park, B.-G., & Handler, G. 2005, A&A, 435, 649
Miksa, S., Deetjen, J. L., Dreizler, S., Kruk, J. W., Rauch, T., & Werner, K. 2002, A&A, 389, 953
Miller Bertolami, M. M., & Althaus, L. G. 2006, A&A, submitted
Miller Bertolami, M. M., Althaus, L. G., Serenelli, A. M., & Panei, J. A. 2006, A&A, in press (astro-ph/0511406)
Montalban, J. 1994, A&A, 281, 421
Morgan, D. H., Parker, Q. A., & Cohen, M. 2003, MNRAS, 346, 719
Mowlavi, N. 1999, A&A, 344, 617
Mowlavi, N., Jorissen, A., & Arnould, M. 1996, A&A, 311, 803
Nagel, T., Schuh, S., Kusterer, D.-J., Stahn, T., Hügelmeyer, S. D., Dreizler, S., Gänsicke, B., & Schreiber, M. 2006, A&A, in press
Napiwotzki, R. 1999, A&A, 350, 101
Napiwotzki, R., & Schönberner, D. 1995, A&A, 301, 545
Napiwotzki, R., Schönberner, D., & Weidemann, V. 1991, A&A, 243, L5
Pandey, G., Lambert, D. L., Jeffery, C. S., & Kameswara Rao, N. 2006, ApJ, 638, 454
Press, W. H. 1981, ApJ, 245, 286
Quirion, P. O., Fontaine, G., & Brassard, P. 2004, ApJ, 610, 436
———. 2005a, A&A, 441, 231
———. 2005b, Mem. Soc. Astron. Italiana, 75, 282
Rauch, T., Dreizler, S., & Wolff, B. 1998, A&A, 338, 651

Rauch, T., Heber, U., Hunger, K., Werner, K., & Neckel, T. 1991, A&A, 241, 457
Rauch, T., & Werner, K. 1995, in White Dwarfs, ed. D. Koester & K. Werner (LNP Vol. 443; Heidelberg: Springer), 186
Reiff, E., Jahn, D., Rauch, T., Werner, K., Kruk, J. W., & Herwig, F. 2006, in ASP Conf. Ser. 349, Astrophysics of Variable Stars, ed. C. A. C. Sterken (San Francisco: ASP), 323
Reiff, E., Rauch, T., Werner, K., & Kruk, J. 2005, in ASP Conf. Ser. 334, White Dwarfs, ed. D. Koester & S. Moehler (San Francisco: ASP), 173
Sackmann, I.-J., & Boothroyd, A. I. 1992, ApJ, 392, L71
Saio, H. 1996, in ASP Conf. Ser. 96, Hydrogen-deficient Stars, ed. U. Heber & C. Jeffery (San Francisco: ASP), 361
Saio, H., & Jeffery, C. S. 2002, MNRAS, 333, 121
Scalo, J. M., Despain, K. H., & Ulrich, R. K. 1975, ApJ, 196, 805
Schönberner, D. 1979, A&A, 79, 108
———. 1983, ApJ, 272, 708
Schönberner, D., & Jeffery, C. S. 2002, in ASP Conf. Ser. 279, Exotic Stars as Challenges to Evolution, ed. C. A. Tout & W. Van Hamme (San Francisco: ASP), 173
Schwarzschild, M., & Härm, R. 1967, ApJ, 150, 961
Seitter, W. C. 1987a, Mitt. Astron. Ges. Hamburg, 68, 244
Seitter, W. C. 1987b, Messenger, 50, 14
Siess, L., Goriely, S., & Langer, N. 2004, A&A, 415, 1089
Smith, L. F., & Aller, L. H. 1969, ApJ, 157, 1245
Starrfield, S., Cox, A. N., Hodson, S. W., & Pesnell, W. D. 1983, ApJ, 268, L27
Straniero, O., Chieffi, A., Limongi, M., Busso, M., Gallino, R., & Arlandini, C. 1997, ApJ, 478, 332
Tylenda, R., Acker, A., & Stenholm, B. 1993, A&AS, 102, 595
Vauclair, G., et al. 2002, A&A, 381, 122
Werner, K. 1992, in The Atmospheres of Early-Type Stars, ed. U. Heber & C. S. Jeffery (LNP 401; Berlin: Springer), 273
———. 1996, A&A, 309, 861
Werner, K., Deetjen, J. L., Dreizler, S., Rauch, T., & Kruk, J. W. 2003, in IAU Symp. 209, Planetary Nebulae: Their Evolution and Role in the Universe, ed. S. Kwok, M. Dopita, & R. Sutherland (San Francisco: ASP), 169
Werner, K., Dreizler, S., Heber, U., Rauch, T., Wisotzki, L., & Hagen, H.-J. 1995, A&A, 293, L75
Werner, K., Hamann, W.-R., Heber, U., Napiwotzki, R., Rauch, T., & Wessolowski, U. 1992, A&A, 259, L69
Werner, K., & Heber, U. 1991, A&A, 247, 476
Werner, K., Heber, U., & Fleming, T. 1994, A&A, 284, 907
Werner, K., Heber, U., & Hunger, K. 1991, A&A, 244, 437
Werner, K., & Koesterke, L. 1992, in The Atmospheres of Early-Type Stars, ed. U. Heber & C. S. Jeffery (LNP 401; Berlin: Springer), 288
Werner, K., & Rauch, T. 1994, A&A, 284, L5
Werner, K., Rauch, T., Barstow, M. A., & Kruk, J. W. 2004a, A&A, 421, 1169
Werner, K., Rauch, T., & Kruk, J. W. 2005, A&A, 433, 641
Werner, K., Rauch, T., Napiwotzki, R., Christlieb, N., Reimers, D., & Karl, C. A. 2004b, A&A, 424, 657
Werner, K., Rauch, T., Reiff, E., Kruk, J. W., & Napiwotzki, R. 2004c, A&A, 427, 685
Wesemael, F., Green, R. F., & Liebert, J. 1985, ApJS, 58, 379
Wood, P. R., & Faulkner, D. J. 1986, ApJ, 307, 659
Young, P. A., Meakin, C., Arnett, D., & Fryer, C. L. 2005, ApJ, 629, L101
Zahn, J.-P. 1991, A&A, 252, 191